AD-A056 866 AERONAUTICAL RESEARCH LABS MELBOURNE (AUSTRALIA) F/G 13/7
A THEORETICAL STUDY OF THE PERFORMANCE OF A NUMBER OF DIFFERENT--ETC(U)
JUL 77 L ERM

UNCLASSIFIED ARL/MECH-ENG-149 NL

1 OF 1
ADA
056866

END
DATE FILMED
9 78
DDC

ARL-Mech-Eng-Report-149

AR-000-734

12

DEPARTMENT OF DEFENCE

DEFENCE SCIENCE AND TECHNOLOGY ORGANISATION

AERONAUTICAL RESEARCH LABORATORIES

MELBOURNE, VICTORIA

MECHANICAL ENGINEERING REPORT 149

A THEORETICAL STUDY OF THE PERFORMANCE OF A NUMBER OF DIFFERENT AXIAL-FLOW TURBINE CONFIGURATIONS UNDER CONDITIONS OF PULSATING FLOW

by

LINCOLN ERM

Approved for Public Release

JULY 1977

COPY No 7

AR-000-734

DEPARTMENT OF DEFENCE
DEFENCE SCIENCE AND TECHNOLOGY ORGANISATION
AERONAUTICAL RESEARCH LABORATORIES

ARL/MECH-ENG-149

Jul 77

55p.

MECHANICAL ENGINEERING REPORT 149

A THEORETICAL STUDY OF THE PERFORMANCE OF A NUMBER OF DIFFERENT AXIAL-FLOW TURBINE CONFIGURATIONS UNDER CONDITIONS OF PULSATING FLOW.

by

LINCOLN/ERM

Technical rept.,

SUMMARY

The work described in this report is a continuation of an earlier investigation aimed at determining the best turbine configuration for operation with the pulsating flow occuring in a constant-volume gas turbine. In the earlier investigation, a radial-inflow turbine was chosen for analysis. This initial work is now extended to a number of different two-stage, axial-flow turbines.

The method of turbine performance prediction for steady-flow operating conditions was developed for a single-stage, axial-flow turbine. During this development it was found that existing correlations for determining turbine loss characteristics at high negative angles of incidence were inadequate and consequently a modified approach had to be developed.

Four basic two-stage turbines, each having different blade angles, as well as several versions of one of these, were chosen for analysis. The mean efficiencies of these machines for pulsating-flow operating conditions were estimated by using a quasi-steady method of analysis. The results obtained for the selected turbines are presented and compared with the results for the radial-inflow turbine. A configuration is proposed that could possibly give better mean efficiencies under pulsating-flow conditions than those actually considered.

POSTAL ADDRESS: Chief Superintendent, Aeronautical Research Laboratories,
P.O. Box 4331, Melbourne, Victoria, 3001, Australia.

DOCUMENT CONTROL DATA SHEET

Security classification of this page Unclassified

1. Document Numbers:
   (*a*) AR Number: 000–734
   (*b*) Document Series and Number:
   Mechanical Engineering Report 149
   (*c*) Report Number:
   ARL/Mech. Eng. Rpt. 149

2. Security Classification:
   (*a*) Complete document: Unclassified
   (*b*) Title in isolation:
   Unclassified
   (*c*) Summary in isolation:
   Unclassified

3. Title: A THEORETICAL STUDY OF THE PERFORMANCE OF A NUMBER OF DIFFERENT AXIAL-FLOW TURBINE CONFIGURATIONS UNDER CONDITIONS OF PULSATING FLOW

4. Personal Author: Lincoln Erm

5. Document Date: July 1977

6. Type of Report and Period Covered: Technical Report

7. Corporate Author(s):
   Aeronautical Research Laboratories

8. Reference Numbers:
   (*a*) Task: DST 76/80
   (*b*) Sponsoring Agency: DSTO

9. Cost Code: 47–7401

10. Imprint: Aeronautical Research Laboratories, Melbourne

11. Computer Program(s):

12. Document Release Limitations: Approved for Public Release

12-0. Overseas: No.		P.R.	1	A		B		C		D		E	

13. Announcement Limitations: No Limitation

14. Descriptors:
   Turbines, Gas Turbines
   Pulsating Flow, Axial Flow Turbines

15. Cosati Codes:
   1307

16.

ABSTRACT

The work described in this report is a continuation of an earlier investigation aimed at determining the best turbine configuration for operation with the pulsating flow occuring in a constant-volume gas turbine. In the earlier investigation, a radial-inflow turbine was chosen for analysis. This initial work is now extended to a number of different two-stage, axial-flow turbines.

The method of turbine performance prediction for steady-flow operating conditions was developed for a single-stage, axial-flow turbine. During this development it was found that existing correlations for determining turbine loss characteristics at high negative angles of incidence were inadequate and consequently a modified approach had to be developed.

Four basic two-stage turbines, each having different blade angles, as well as several versions of one of these, were chosen for analysis. The mean efficiencies of these machines for pulsating-flow operating conditions were estimated by using a quasi-steady method of analysis. The results obtained for the selected turbines are presented and compared with the results for the radial-inflow turbine. A configuration is proposed that could possibly give better mean efficiencies under pulsating-flow conditions than those actually considered.

CONTENTS

1. INTRODUCTION

The present theoretical work is a continuation of earlier work by Erm (1973) aimed at determining the best turbine configuration for operation with pulsating flow from a constant-volume combustor. Theoretical studies had indicated that for small gas turbines, certain significant thermodynamic advantages might well be gained if the combustion takes place at constant volume rather than at constant pressure. In the earlier work, a single-stage radial-inflow turbine was chosen for analysis. Here some two-stage, axial-flow turbines are examined.

Two-stage machines were chosen for analysis because they are the simplest form of a multi-stage turbine which will generally be required in practice. Two stages would suffice to indicate whether variation of mean flow angles between early and later stages during pulsating-flow operation would warrant some biasing of blade angles to improve the mean efficiency.

The method of turbine performance prediction was developed by examining a single-stage turbine. The steady-flow performance of this machine was compared with the measured performance of a similar turbine; the comparison indicated that existing methods for determining turbine loss characteristics at high negative angles of incidence were unsatisfactory. As a consequence, a modified approach had to be developed. The initial analysis was extended to the two-stage turbines thereby enabling their steady-flow performance to be determined. The mean efficiencies of these turbines under pulsating-flow operating conditions were then estimated using a quasi-steady method of analysis. Further, due to the inertia of rotating parts, fluctuations of rotational speed arising from the pulsating flow could be ignored in this investigation.

The study has been concerned with a comparison of the mean efficiencies of the turbines under pulsating-flow conditions rather than with their work outputs. These mean efficiencies affect the performance of a constant-volume gas turbine in a similar way that the equivalent steady-flow efficiencies affect the performance of a more conventional constant-pressure gas turbine.

2. DEVELOPMENT OF METHOD OF TURBINE PERFORMANCE PREDICTION FOR STEADY-FLOW OPERATING CONDITIONS

The development of a method of performance prediction of a single-stage turbine for steady-flow operating conditions is described below.

2.1 Details of Turbine Geometrical and Loss Characteristics

The geometrical and loss characteristics of the turbine are first considered. The stator and rotor, together with general velocity diagrams, are depicted in Fig. 1 in order to indicate the locations of the various stations along the flow path together with the sign convention adopted for flow and blade angles.

2.1.1 Selection of Turbine Blade Characteristics at Reference Diameter

In order to operate efficiently with pulsating flows, a turbine should have a high efficiency over a wide range of velocity ratios. As a preliminary approach it was thought desirable to select a turbine blading geometry known to give a high steady-flow, design-point efficiency, together with any features known to reduce the tendency for losses to increase under off-design conditions.

Optimisation of the design-point performance is assisted by published parametric studies by Hawthorne (1957), Shaw (1964) and Smith and Johnston (1967). The first two of these studies are summarised by Horlock (1966). These studies indicate that losses in the blading are minimised by choice of a stage reaction of about 50%, and stator and rotor outlet blade angles of about 60°.

At off-design conditions, an additional source of energy loss arises from the flow entering the rotor at some (positive or negative) incidence angle. It has been shown (e.g. Emmert (1950)) that this loss is less for rotor blades with a large nose radius than for those with a small nose radius, so that the former are to be preferred for pulsating flow.

Further, the analytical work of Ainley and Mathieson (1951) showed that reaction-type rotor blading with approximately axial inlet blade angles and relatively high outlet blade angles gives less increase in loss with incidence angle than does impulse-type rotor blading; blades of this type also satisfy the above requirements for optimum design-point performance.

This indicates that if the stage loading coefficient, Ψ, is selected to be about 1·0 then blading of this type should give a reasonable combination of design-point efficiency, stage loading and insensitivity to off-design operation. In order to select other blade characteristics the work of Ainley and Mathieson (1951) was used as a guide. The selected blade characteristics at the reference diameter are set out in Table I.

A cross section of a pair of turbine blades is shown diagramatically in Fig. 2 in order to indicate turbine blade nomenclature. The selected blade shape is shown in Fig. 3. The blade was chosen to have a T6 profile (Ainley (1948)) on a parabolic camber line, which matched the selected blade angles, and $t_{max}/c = 0{\cdot}200$. Also shown in Fig. 3 are the selected design-point velocity diagrams. The velocities, which are determined in Section 2.1.3, are relatively low in order that the flow in the blade passages under peak pressure conditions remains subsonic. It is assumed that both rows of blading are designed to give a 60° outlet flow angle at the design point, and that this flow angle is maintained under all conditions.

2.1.2 Analysis and Calculation of Turbine Loss Characteristics

To calculate the loss characteristics for the chosen turbine configuration, it is necessary to establish the most appropriate correlation upon which to base the losses. Investigators have proposed axial turbine loss correlations in terms of blade geometry and other factors. Those of Soderberg (1949) and Ainley and Mathieson (1951) appear to be the most authoritative: the latter takes into account the effects of a greater range of design and operating variables and is applicable at off-design conditions, whereas the former correlation is essentially applicable at design-point conditions only. Since pulsating flows involve continual variation of operating conditions, the correlation of Ainley and Mathieson was considered to be the more appropriate. However, a revised form of this correlation, as proposed by Dunham and Came (1970), incorporates several improvements which result from the analysis of more recent turbine data, and has been adopted for use in the current investigation.

Verification of the validity of the revised Ainley and Mathieson correlation (generally referred to as the revised Ainley correlation in the remainder of this report) is given by Dunham and Came (1970) and Dunham and Panton (1973) who compared predictions with experimental results. It should be realised, however, that most of the experimental verification appears to be related to operation at positive or low negative angles of incidence (as defined in Fig. 2), so that the accuracy of this correlation at large negative angles of incidence has not been subjected to an experimental check.

In the revised Ainley correlation, the blade row losses are expressed as a coefficient relating the decrement in total pressure to the dynamic pressure at outlet from the blade row. The total loss coefficient for a particular blade row, say 123 (refer to Fig. 1), is given by $Y_{T13} = (P_1 - P_3)/(P_3 - p_3)$. This coefficient is considered to represent the sum of component losses due to blade profile, secondary flows and blade tip clearance.

The profile loss of a turbine blade is the loss due to boundary layer growth on the blade surface and dissipation in the blade wake, and is a function largely of blade and flow angles. The secondary losses are due to interaction between the blade surface flow and the boundary layers on the end walls and thus depend mainly on aspect ratio and blade loading. The tip clearance loss is the increase in end loss due to clearance and is a function of blade loading and the size and nature of the clearance.

The details of the calculation of the component loss coefficients for the selected blade geometry, under a wide range of flow conditions, are given in Appendix II. The variation of component and total loss coefficients with incidence angle, for the rotor, are shown in Fig. 4.

Superimposed upon this figure is a curve showing rotor loss coefficients as determined by a modified correlation, in an attempt to improve the agreement between the predicted performance of the current turbine and the actual performance of a typical turbine at high negative incidence angles. The need for this modification, and how it was obtained, are set out in Sections 2.3 and 2.4 respectively.

2.1.3 Calculation of Turbine Flow Areas

Before the flow areas throughout the single-stage turbine could be calculated, it was first necessary to select appropriate design-point conditions by analysing the likely flow conditions within a constant-volume gas turbine. Preliminary cycle calculations, as summarised by Williams (1975), indicated that a typical engine cycle could involve pressure pulsations in the combustor between 3 and 9 times atmospheric pressure, with a mean turbine inlet temperature of 1200 K. Also, since an engine of about 150 kW output is envisaged and since the rig test turbine is likely to be operated at reduced temperature, say 600 K mean, then the following design-point conditions were chosen.

ENGINE TURBINE	RIG TURBINE
$T_1 = 1200$ K	$T_1 = 600$ K
$P_1 = 620$ kPa	$P_1 = 620$ kPa
$\dot{m} = 0{\cdot}907$ kg/s	$\dot{m} = 1{\cdot}283$ kg/s
$M_3 = 0{\cdot}6$	$M_3 = 0{\cdot}6$

The turbine design calculations were based upon the expected rig turbine conditions. The calculations were performed by using the above chosen design-point conditions together with the selected shapes for the design-point velocity diagrams as given in Fig. 3 and the loss coefficients appropriate to each blade row at the design condition as given in Fig. 4, and working through the turbine in a step-by-step manner.

Flow conditions and flow areas at all stations throughout the turbine are given in Table II.

2.2 Prediction of Turbine Efficiency

The efficiency of the single-stage turbine was predicted for a wide range of operating conditions, thereby enabling the predicted performance of this machine to be compared with the measured performance of a similar, existing unit.

Values of efficiency can be determined as a function of either inlet total pressure and outlet static pressure or inlet total pressure and outlet total pressure. The former specification of efficiency is probably the more appropriate to use in the current investigation since operation with constant outlet static pressure is likely to be typical of a constant-volume gas turbine, since efficient outlet diffuser operation under pulsating flow conditions is very unlikely.

A broad outline of the thermodynamic analysis associated with the prediction of turbine efficiencies is presented in this section. Details of the equations used and the techniques adopted are given in Appendix III.

When predicting efficiencies for specified operating conditions the flow conditions at the reference diameter are established by using conventional one-dimensional thermodynamic methods. The blade row losses are determined by using the loss characteristics given in Fig. 4, with due consideration of the incidence angle at the rotor inlet for the particular operating conditions. A feature of the analysis is that it is quite general and is applicable to both subsonic and supersonic flow conditions in the turbine.

In order to establish the flow for the chosen operating conditions, viz. T_1, P_1, p_7 and U, it is necessary to adopt an iterative approach. This process involves systematically choosing trial values of p_3 and evaluating the flow variables through the turbine until the mass flow rates through the stator and rotor agree within defined limits. It is then possible to determine the turbine efficiency. A digital computer has been programmed to facilitate the calculations.

2.3 Comparison of Predicted Efficiencies with Published Data

The validity of the method used to predict turbine efficiencies may be assessed by comparing values of efficiency predicted by this method with appropriate published experimental data.

The validity of the revised Ainley correlation for operation at normal design-point conditions, i.e. with negligible incidence angle at the rotor inlet, has been demonstrated by Dunham and Came (1970) and Dunham and Panton (1973). This means that the accuracy of prediction of the maximum efficiency (i.e. the peak of the efficiency-velocity ratio characteristic curve) is not now in question, but there is a need in the present investigation to check that the use of the revised Ainley correlation leads to a realistic shape for the remainder of the characteristic curve.

Unfortunately, there is very little published experimental data covering the wide range of velocity ratio which has to be considered in a constant-volume gas turbine application. Panton (1967) and Dunham and Panton (1973) present suitable data for a series of small, single-stage experimental turbines. None of the configurations tested had exactly the same blade angles as those selected (see Section 2.1.1) for the turbine considered in the current investigation: their turbine A had a mean rotor outlet angle of 72° and turbine C a mean rotor outlet angle of 60°, while both turbines had a mean stator outlet angle of 66°. These turbines gave differing peak efficiencies; that for turbine C was within one percentage point of that predicted for the turbine currently being investigated. However, the shape of the efficiency-velocity ratio characteristic curve for both of these experimental machines is the same when compared on a normalised basis (i.e. efficiency/peak efficiency plotted against velocity ratio/velocity ratio for peak efficiency). Since these two turbines have a normalised characteristic curve of the same shape even though geometrical differences exist between them, it is reasonable to believe that the slight geometrical differences between the present turbine and turbines A and C should not introduce any significant variation in the shape of the normalised characteristic curve.

The operating conditions for which the efficiencies were predicted were chosen to cover a wide range of velocity ratios. This was achieved by keeping values of T_1, P_1 and p_7 constant at their design-point values and varying the value of U over the range from 37% to 247% of its design-point value in regular steps. All details of the chosen operating conditions together with some of the derived flow conditions as well as the predicted values of efficiency are shown in Table III. The normalised values of efficiency and velocity ratio are superimposed upon the characteristic curve for turbine A in Fig. 5 so that a comparison could be made between the predicted and experimental results (also shown on this figure are values of efficiency predicted by using the modified correlation—see Section 2.4).

It is clear from the comparison that the predicted values of efficiency based upon the revised Ainley correlation give a characteristic curve of the correct shape at low velocity ratios (i.e. positive incidence angles at the rotor inlet) but have resulted in optimistic efficiencies at high velocity ratios (i.e. high negative incidence angles at the rotor inlet). This indicates that the loss coefficients given by this correlation for high negative incidence angles (e.g. $-20°$ to $-60°$) are too low. These values occur because the secondary and tip clearance formulae express the losses as a function of the overall flow deflection through the blade row, and this tends to zero at $i = -60°$ for this particular blading. In the practical situation, however, at this condition, the flow probably separates and deflects on entering the blade row, and then deflects equally the other way in the blade passages: the extra losses associated with this flow condition are not taken into account in the revised Ainley correlation.

Unfortunately, no more satisfactory method for determining secondary and tip clearance loss characteristics is offered in the literature, so that it is necessary to modify the total loss coefficient for negative angles of incidence.

2.4 Modification of Turbine Loss Characteristics at Negative Incidence Angles

If the alternative loss correlation of Soderberg (1949), as summarised by Horlock (1966), is reconsidered, then the data offered concerning incidence effects is limited in scope but suggests that, for blades of the thickness considered, the total loss is at its minimum at about zero incidence angle, and may be greater at negative incidence angles than at the corresponding positive incidence angles. Emmert (1950) showed that round nosed blades had slightly greater losses at negative incidence angles than at equivalent positive incidence angles, whereas the opposite trend was noticed for sharp nosed blades. Kroon and Tobiasz (1971) analysed experimental data to determine the effects of incidence on blading efficiency, and showed that the pressure loss due to incidence could be approximated by a function of $\tan^2 i$, which is symmetrical about $i = 0°$.

Since the revised Ainley correlation is believed to be accurate at zero and positive incidence

angles, it was decided to retain it as the basic correlation, but modify the total loss coefficient curve for the rotor to the form $Y_{T46} = K \tan^2 i_4 + Y_{T46(0)}$ in order to conform more closely with the loss characteristics noted above. The modified curve was fitted to the revised Ainley curve at $i_4 = 0°$ and $i_4 = +30°$, to give similar results for positive angles of incidence. It is shown in Fig. 4 where it is superimposed upon the corresponding revised Ainley curve determined in Section 2.1.2.

In order to assess the accuracy of the modified turbine rotor loss characteristics, it was necessary to perform a checking procedure similar to that outlined in Section 2.3. For chosen operating conditions, a number of values of efficiency were predicted by using the efficiency-prediction method outlined in Section 2.2, but with the turbine rotor loss characteristics determined by the modified correlation instead of the revised Ainley correlation. The chosen operating conditions, which are the same as those used in Section 2.3, are shown in Table III together with the predicted values of efficiency. The normalised values of efficiency and velocity ratio are superimposed as before upon the characteristic curve for turbine A as shown in Fig. 5 so that a comparison could be made between the predicted and experimental results. It is evident from the comparison that the increased losses at negative angles of incidence have depressed the efficiency at high velocity ratios further than was required to match the actual performance of the experimental turbine.

As the normalised characteristic curve for the experimental turbine falls approximately midway between the predicted curves based on the revised Ainley and the modified correlations respectively, it was decided to proceed with the investigation using both correlations to determine turbine loss coefficients. In this way two estimates of the effect of any geometrical change would be obtained, the difference between them indicating the degree of uncertainty due to imprecision in the determination of loss coefficients, and the mean of the two values giving some estimate of the effect likely to be expected in practice. This was felt to be preferable to further modifying the total loss coefficient curve for the rotor so that agreement with practical results was obtained, which could lead to performance assessments being made without any idea of the uncertainties involved.

It is clear that a better knowledge of turbine loss characteristics at high negative angles of incidence will be needed before accurate optimisation of geometry for pulsating flows can be attempted.

3. ANALYSIS OF TWO-STAGE TURBINES FOR STEADY-FLOW OPERATING CONDITIONS

The method of analysis used for the single-stage turbine was extended to predict the performance of the two-stage turbines for steady-flow operation.

3.1 Details of Turbine Geometrical and Loss Characteristics

In this investigation four different configurations of two-stage turbine were chosen for analysis.

3.1.1 Selection of Turbine Blade Characteristics at Reference Diameter

The four turbines considered differ only in blade angles, other geometrical features being the same as for the single-stage turbine. In each case, both stages have the same outlet blade angles and are designed to give identical velocity diagrams. The selected turbine blade characteristics at the reference diameter are set out in Table IV.

Build 1 retained the blade angles of the single-stage machine as a basic configuration while the other three have variations of blade angle from this datum in order to assess the effects of such changes on efficiency, since these changes alter both the sensitivity of the blading loss characteristics to incidence angle variation and the range of incidence angles encountered by the blading during a given pulse. These effects are demonstrated in Fig. 6 which depicts the variation of the total loss coefficients with incidence angle for the rotor blades of each turbine (see Section 3.1.2), and also shows how the velocity diagrams vary from the beginning to the end of the standard pulse considered later in Section 4.

To simplify the presentation, only the velocity diagrams appropriate to loss calculations based on the revised Ainley correlation are given: loss calculations based on the modified correlation lead to slightly different flow angle variations during the cycle.

The range of incidence angles encountered for the standard pulse are indicated on the velocity diagrams as well as on the corresponding loss curves by shaded regions. It can be seen that Build 2, with reduced blade outlet angles, experiences a smaller variation in rotor incidence angle in the vicinity of the design point than Build 1, but the loss coefficient is more sensitive to incidence angle changes. Build 3, with increased blade outlet angles, has a greater variation in rotor incidence angle, but the loss coefficient is less sensitive to incidence angle changes. Build 4, with non-axial rotor inlet angles, is another configuration with a smaller variation in rotor incidence angle but with a loss coefficient that is more sensitive to incidence angle changes.

It was considered that these four configurations would serve to indicate how blade angles should be optimised for pulsating flow.

3.1.2 Calculation of Turbine Loss Characteristics

The blading loss characteristics for the four turbine configurations were calculated by using both the revised Ainley and the modified correlations.

The method used to calculate the loss characteristics using the first correlation is similar to that detailed in Appendix II for the single-stage turbine.

For the second correlation, relationships of the form $Y_T = K \tan^2 i + Y_{T(0)}$ were fitted to the appropriate revised Ainley curves at $i = 0°$ and $i = +30°$, as before, for each configuration of rotor. Instead of fitting curves in this manner for the second stators, an approximate method was used in which the loss curves for the rotors were factored down to give the correct loss coefficients for the second stators at $i_7 = 0°$, the loss coefficients at all other angles of incidence being reduced in the same proportion.

For Build 4, a variation was adopted in deriving the loss curves corresponding to the modified correlation, since for non-axial blade inlet angles the limits of incidence angle are not symmetrical with respect to $i = 0°$. In this case, different equations were used for positive and negative incidence angles, i.e. $Y_T = K \tan^2 (i \times 90/60) + Y_{T(0)}$ and $Y_T = K \tan^2 (i \times 90/120) + Y_{T(0)}$ respectively.

The loss curves derived by both of these correlations for the four configurations are shown in Fig. 6 for the first stators and the rotors only. The curves for the second stators, corresponding to both correlations, have been omitted from this figure in order to avoid confusion. They are of similar shape but slightly below the appropriate rotor curves.

3.1.3 Calculation of Turbine Flow Areas

For the two-stage turbines, the design-point values of T_1, P_1 and $\dot{m}$, used in calculating the turbine flow areas, were identical to those used in Section 2.1.3 for the single-stage machine. The design-point velocity diagrams selected for the four turbine configurations are shown in Fig. 6. In these diagrams two requirements were satisfied; one was that the inlet flow was at zero incidence and the other was that each stage of each two-stage machine gave the same work as the single-stage turbine. Builds 1 to 3 have a stage loading coefficient of 1·0, therefore the blade speed for these three turbines is the same. Build 4, with non-axial inlet flow, has a stage loading coefficient of 2·0, so the blade speed is reduced to $1/\sqrt{2 \cdot 0}$ times that of the other turbines.

The design calculations for each turbine were performed using the above selected design-point conditions and velocity diagrams as well as the loss coefficients appropriate to each blade row at the design condition. The method used is an extension of that used for the single-stage turbine and does not require further description. Table V summarises the flow conditions and flow areas at all stations throughout each turbine.

3.1.4 Redistribution of Flow Angles by Area Changes

Under pulsating-flow conditions it is found that the different blade rows of each particular turbine are subjected to different mean inlet flow angles. Since the inlet blade angles on the

latter three blade rows of each particular turbine are the same, the matching of the flow to the blades throughout the turbines is not necessarily optimum. Consequently gains in mean efficiency may be possible if the matching throughout the turbines is improved.

In an attempt to obtain improved mean efficiencies, the flow areas through the turbine were changed, thereby redistributing the flow directions and thus altering the matching. This procedure was relatively simple and involved only minor changes to the efficiency-prediction programme (referred to in Section 3.2). In the current investigation only the flow areas of Build 1 have been changed. Altogether seven different versions of this build were investigated. They were obtained by decreasing (or increasing) the flow areas at the turbine inlets and correspondingly increasing (or decreasing) the flow areas at the turbine outlets and changing the flow areas at the intermediate locations by proportional amounts. The details of the different versions are shown below.

	Change of flow areas at turbine inlet (station 1) %	Change of flow areas at turbine outlet (station 12) %
Version 1	0	0
Version 2	−10	+10
Version 3	−20	+20
Version 4	− 5	+ 5
Version 5	−15	+15
Version 6	+10	−10
Version 7	+20	−20

It is to be noted that due to the bulkiness of the complete set of results associated with all of the versions, only a representative sample is presented here.

3.2 Prediction of Turbine Efficiency

The method used to predict the efficiencies of the two-stage turbines for specified operating conditions, T_1, P_1, p_{13} and U, is an extension of that outlined in Section 2.2 and Appendix III for the single-stage turbine.

The iterative process used to establish the flow conditions throughout these turbines is slightly more complex than that used for the single-stage machine since in this case three pressures have to be determined by iteration. For an arbitrarily selected value of p_7 a series of values of p_3 are systematically chosen until the mass flow rates through the first stator and first rotor agree within defined limits and also, for the same value of p_7, a series of values of p_9 are systematically chosen until the mass flow rates through the second stator and second rotor agree within similar limits. The mass flow rates through the first and second stages are then compared and if there is a large discrepancy then the value of p_7 is modified and the entire procedure repeated until the mass flow rates through both stages agree within the defined limits. When this occurs, all other flow variables form a balanced solution for the chosen operating conditions and it is then possible to determine the turbine efficiency.

3.3 Prediction of Steady-Flow Efficiencies for Operating Conditions Encountered Momentarily by Turbines During Pulsating Flow

When the turbines are operating under pulsating-flow conditions their efficiencies are continually changing because of continual changes in the operating conditions. The efficiency-prediction method outlined in the previous section was used to predict the efficiencies of the two-stage turbines for a number of discrete sets of operating conditions encountered by the turbines during pulsating-flow operation.

A representative sample of the chosen operating conditions for which the efficiencies were predicted is given in Table VI for Build 1. The inlet temperatures and pressures are typical combinations obtained from a preliminary analysis of a turbine operating under a selected type of pulsating flow (see Section 4.2 and Fig. 9). The blade speeds correspond to the design speed and the outlet pressures correspond to atmospheric pressure. The predicted values of efficiency together with corresponding values of velocity ratio are also given in Table VI. The

efficiencies and velocity ratios have been computed as a function of inlet total pressure and outlet total pressure and also inlet total pressure and outlet static pressure for the cases when the turbine loss characteristics are determined by both the revised Ainley and the modified correlations. The data contained in Table VI are shown plotted in Fig. 7 together with similar plots for the other turbines.

In order to establish simplified mathematical relationships between η and ν for use in the pulsating-flow analysis, and thus avoid frequent resort to the detailed turbine flow analysis described in Section 3.2, the curves shown in Fig. 7, which correspond to typical constant-volume operating conditions, were fitted by the method of least squares.

To be able to select an optimum blade speed for each turbine, the above procedure was repeated for two additional speeds, all other operating conditions remaining unchanged. The additional speeds were 25% above and 25% below the design speeds.

The procedure described above for Builds 1 to 4 was extended to the different versions of Build 1. The operating conditions, efficiencies and velocity ratios, as well as the efficiency-velocity ratio curves, associated with the different versions of Build 1 are not documented, however, since they are basically the same as those already presented.

4. ESTIMATION OF TURBINE MEAN EFFICIENCY UNDER PULSATING-FLOW CONDITIONS

In the preceding work the two-stage turbines have only been analysed for steady-flow operating conditions. The analysis is now extended to the more complex case of pulsating flow. Estimates are made of the mean efficiencies of the different two-stage turbines when they are operating under pulsating-flow conditions similar to those that occur in a constant-volume gas turbine.

The unsteady flow used in the current investigation is defined primarily in terms of a form of cyclic pressure fluctuation in the combustor (i.e. at the turbine inlet). The form of the idealised pressure pulse chosen for analysis is depicted in Fig. 8 for a complete cycle. As can be seen from this figure, the pulsed cycle is conveniently divided into three distinct parts, namely pressure rise (combustion), blowdown and scavenging. Instantaneous pressure rise due to combustion is depicted in the figure although for more accurate simulation extra time for combustion could be added to the cycle time. During the blowdown phase there is no cold scavenge air flowing into the combustor from the compressor and the pressure continually decreases with time, as shown, as the hot gas is discharged through the turbine. During scavenging the cold incoming air is assumed to intermix completely with the hot, undischarged combustor contents and the pressure in the combustor remains essentially constant.

In order to define the pulsating flow more precisely it is necessary to specify certain basic cycle features. In an earlier study on a radial-inflow turbine by Erm (1973), a pulse corresponding to a compressor pressure ratio of 2·85 :1 and a combustion pressure ratio of 3·00 :1, making a peak pressure ratio of 8·55 :1, was used. Since this pressure ratio would result in choking in a two-stage turbine (probably three stages would be needed in practice for this pressure ratio), a pulse corresponding to a compressor pressure ratio of 1·71 :1 and a combustion pressure ratio of 2·34 :1, giving a peak pressure ratio of 4·00 :1, was used. These compressor and combustion pressure ratios were chosen since they led to approximately the same ratio of velocity ratio for the two-stage turbines, i.e. the final value is 2·34 times the initial value (expressed as a function of inlet total pressure and outlet static pressure), as for the radial-inflow turbine mentioned above, thus maintaining a comparable severity of pulsation. Variables associated with the pulse depicted in Fig. 8 as well as the turbines' speeds are listed below.

p_{0v} = 173·3 kPa
p_{0w} = 405·6 kPa
p_{13} = 101·4 kPa
U = 184·8, 246·5, 308·1 m/s (Builds 1 to 3) (Build 1, Versions 1 to 7)
U = 130·7, 174·3, 217·8 m/s (Build 4)
P_{SCAV} = 173·3 kPa
T_{SCAV} = 359·1 K

The reasoning behind the selection of values for p_{0v} and p_{0w}, the pressures in the combustor

before and after combustion respectively, has already been given. The values of U correspond to the design speeds and speeds 25% above and below the design speeds. The values of P_{SCAV} and T_{SCAV} correspond to the pressure and temperature respectively of the scavenging air after the air has been compressed from atmospheric conditions through a pressure ratio of 1·80:1 and has undergone a charging pressure loss of 5%. The combustor volume, v_0, was chosen to be 0·0566 m³ (2·0 ft.³), the same as that used for the radial-inflow turbine. The values of total temperature and pressure at the turbine inlet are taken to be equal to their respective static values within the combustor.

As was done for the radial-inflow turbine, the pulsating flow in the current investigation was analysed by using a quasi-steady approach. In order to do this it was necessary to subdivide the pulsed cycle into a number of intervals, each corresponding to a time increment, Δt, in the manner shown in Fig. 8. Uniform intervals need not necessarily be used, but for simplicity they were used here. It was assumed that the combustor pressure and temperature remained constant for the duration of these short time intervals. The justification for analysing the pulsating flow in this manner is discussed in Section 5.2.2.

The pulsating-flow analysis is simplified by assuming that all flow is one-dimensional and that the specific heats of the gas do not vary with temperature. In order to simplify the presentation, only a broad outline of the analysis is given in this section. Further details are given in Appendix IV. Both the blowdown and scavenging phases of the pulsating flow are analysed thermodynamically and then the method used to estimate the mean efficiency of a turbine when it is operating under pulsating-flow conditions is described.

4.1 Blowdown Phase

Before the blowdown calculations can be commenced, it is first necessary to select a trial value of t_{0V}, the combustor temperature before combustion. It will generally be necessary to modify this value of t_{0V} at a later stage if it does not agree with the computed combustor temperature at the end of the scavenging phase.

The mass of gas in the combustor at the start of blowdown can be determined from the initial pressure, temperature and volume. A pseudo mass flow rate can be determined by using these initial conditions (see Appendix IV for details) and from this mass flow rate it is possible to determine the mass outflow during the first time interval. The actual increment of turbine work in the interval can be determined by first computing the isentropic increment of work from a knowledge of the increment of mass flow, the gas temperature and pressures, and then multiplying the result by the turbine efficiency. The efficiency can be determined by computing the velocity ratio, which depends upon the initial temperature and pressures as well as the speed, and then using the appropriate efficiency-velocity ratio relationship shown in Fig. 7.

At the end of the time interval, the residual mass of gas in the combustor can be determined and the new pressure and temperature calculated assuming that the combustor contents have expanded isentropically to the new condition. These new conditions become the initial conditions for the following interval. The procedure can be repeated for successive time intervals until the combustor pressure falls to, or below, the scavenging pressure, P_{SCAV}, at which point the scavenging process is commenced.

Throughout the blowdown process the isentropic work increments and the actual turbine work increments are summated, with the view of obtaining totals for the whole cycle from which the mean efficiency can be calculated.

4.2 Scavenging Phase

The scavenging calculations are very similar to those outlined above for the blowdown phase. In this case, however, an allowance has to be made for the effects of the incoming scavenging air.

For the first time interval of the scavenging phase the turbine entry conditions are equal to those at the end of blowdown and the mass outflow and the isentropic and actual increments of work can be determined by using the method outlined above for the blowdown phase. During the interval, the volume outflow is replaced by an equal volume of entering scavenging air. At the end of the time interval, the mass of gas in the combustor can be determined and the

temperature of the mixture calculated on the assumption that the cold incoming air intermixes completely with the hot undischarged combustor contents. This new temperature becomes the initial temperature for the following interval.

The procedure can be repeated for successive time intervals until scavenging is terminated at the point where a specified mass of cold scavenging air has entered the combustor. This mass was chosen to be equal to the mass contained within the combustor at scavenging pressure and temperature (as for the radial turbine).

Throughout the scavenging process the isentropic work increments and the actual work increments are summated and added to those for the blowdown phase to obtain totals for the cycle.

At the end of the scavenging phase, a comparison is made between the final value of t_0, the combustor temperature, and the trial value of t_{0v} selected at the start of the blowdown analysis. If there is a large discrepancy between these two values of temperature, then the value of t_{0v} is modified and the cycle calculations repeated until the agreement is acceptable.

Table VII lists a number of flow characteristics at various stages throughout a pulsating-flow cycle. The data presented in Table VII are only a representative sample of the results obtained, and correspond to Build 1 when it is operating at the design speed and when the turbine loss characteristics are determined by the modified correlation. The combustor pressure, temperature and mass listed in Table VII are shown plotted in Fig. 9. The twenty three pressure-temperature combinations which were used when predicting turbine efficiencies (see Section 3.3) are clearly indicated on this figure. A number of corresponding turbine internal flow characteristics, most of which are not listed in Table VII, are shown plotted in Fig. 10. Detailed discussion on this figure is given in Section 5.

4.3 Estimation of a Mean Turbine Efficiency

Now that both the blowdown and scavenging phases of the pulsed cycle have been analysed thermodynamically it is possible to estimate the mean total-static efficiencies of the turbines when they are operating under pulsating flow. The mean efficiency is simply the ratio of the sum of the actual work increments to the sum of the isentropic work increments for the whole cycle.

The mean total-static efficiencies of Builds 1 to 4 when they are operating at 75%, 100% and 125% of their design speeds and when their loss characteristics are determined by both the revised Ainley and the modified correlations, are shown in Fig. 11. The maximum mean total-static efficiency that could reasonably be expected in practice for the pulsating flow considered is approximately 75·6% and would be obtained by Build 3 when operating at about its design speed.

The mean total-total and the mean total-static efficiencies of Build 1, Versions 1, 3 and 6, when they are operating at the design speed of Build 1 and when their loss characteristics are determined by the modified correlation, are shown in Fig. 12.

Discussion on the above results is given in Section 5.

5. DISCUSSION

A method of turbine performance prediction for steady-flow operating conditions has been developed initially for a single-stage turbine and extended to a number of different two-stage turbines thereby enabling their steady-flow performance characteristics to be determined. Once the steady-flow behaviour of these turbines is known, then their mean efficiencies when operating under a selected type of pulsating flow can be estimated.

In this work a number of factors arose which require examination in order to assess their effects upon the validity of the conclusions. The discussion of these factors is grouped into sections which deal with the steady-flow and pulsating-flow operation of the turbines respectively and also a section that compares the estimated mean efficiencies of the axial-flow turbines with those of a radial-inflow turbine (Erm (1973)).

5.1 Steady-Flow Operating Conditions

Various aspects of the analysis associated with the steady-flow operation of the turbines are now considered.

5.1.1 Turbine Loss Characteristics

When the theoretically predicted values of efficiency for the single-stage turbine were compared with corresponding data of Panton (1967) significant differences between the two sets of results for operation at high negative angles of incidence suggested that the revised Ainley correlation is inadequate to determine the turbine loss characteristics in this region of operation. One possible explanation for these differences in efficiency is that the turbines used in the comparison are not identical. However, this explanation can be discounted since it was shown in Section 2.3 that two turbines, somewhat similar to the single-stage turbine considered in this investigation, had a normalised efficiency-velocity ratio characteristic curve of the same shape even though definite geometrical differences existed between them.

In an attempt to obtain better agreement between theoretical and experimental results, the rotor loss characteristics of the single-stage turbine were modified to the form $Y_T = K \tan^2 i + Y_{T(0)}$. Justification for modifying the turbine loss characteristics in this manner is given in Section 2.4. A comparison of predicted and actual performance showed that the modified correlation was also inadequate to determine the turbine loss characteristics at high negative angles of incidence; in fact the use of the modified correlation overcorrected the efficiency disparity and led to efficiencies as far removed from the experimental normalised characteristic curve as initially.

It is clear from the above that the exact form of the loss characteristics of the single-stage turbine considered in this investigation at high negative angles of incidence is not known; however, it could be expected that the losses are about midway between those determined by using both correlations. Consequently it was decided to proceed with the planned investigation using both correlations since by doing this at least the limits would be obtained of the true turbine behaviour to be expected in practice. Some justification for doing this is given in Section 2.4. It is to be emphasised that very little experimental investigation of turbine operation at high negative angles of incidence has been reported, and therefore the exact nature of turbine loss characteristics in this region of operation is uncertain. More data are needed before reliable optimisation of turbine geometry for pulsating-flow operation can be attempted.

5.1.2 Prediction of Turbine Efficiency

The use of a simplified analysis in the current investigation raises the question whether or not the results obtained are reliable. A simplified analysis, similar to that used in this investigation, was used by Dunham and Came (1970), who compared predicted values of efficiency of twenty five turbines with corresponding experimentally measured values. The predicted values of efficiency were within 2% of the corresponding experimentally measured values except in a few cases. The good agreement between predicted and measured efficiencies obtained by these workers by using a simplified thermodynamic analysis gives confidence in the accuracy of the predicted values of efficiency obtained in the current investigation.

5.2 Pulsating-Flow Operating Conditions

Various aspects of the analysis associated with the pulsating-flow operation of the turbines are now considered.

5.2.1 Idealised Flow into Turbine

The flow into the turbine is idealised and is based upon a number of approximations which have been discussed.

The use of this idealised pulsating flow provides a simple means of making a comparison between the unsteady and steady performances of a particular turbine. Similarly, it is possible to compare the unsteady performance of different turbines.

5.2.2 Quasi-Steady Method of Analysis

The pulsating flow used in the current investigation was analysed by using a quasi-steady method. This means that the unsteady flow conditions existing throughout the turbines were approximated by a series of steady-flow processes. Although not as desirable as a more rigorous treatment, this was a tractable way of dealing with the physics of pulsating flow. The question does arise, however, of the accuracy of this approach.

A justification for use of the quasi-steady method of analysis is that the rate of change of the turbine inlet conditions is slow enough that the inlet conditions do not change significantly during the time required for a particle of gas to pass through the turbines. For the two-stage turbines operating at optimum velocity ratio, with typical temperatures and pressures, this time is of the order of 1 ms.

Furthermore, as indicated by Horlock (1968), the value of the frequency parameter, given by $\omega = (\text{frequency} \times \text{blade chord})/(2 \times \text{mean velocity})$, can be used to assess the accuracy of a quasi-steady method of analysis. For the present investigation the value of the frequency parameter for the four turbines is in the region of 0·01. Horlock (1968) indicates that quasi-steady analyses appear to be of value at these values of frequency parameter.

It is also essential that the time intervals used in the calculations are kept small enough that the turbine inlet conditions do not change excessively from one time interval to the next. In the current investigation, the time intervals were chosen to be 0·001 s. Table VII lists selected data at 0·010 s intervals.

It is apparent from Table VII and Fig. 9 that the above two requirements are satisfied. Any inaccuracies resulting from the use of this method will primarily be due to the regions of more rapid temperature and pressure change. The possible inaccuracies will be minimised, however, due to the fact that these regions are only a small portion of the total cycle period.

5.2.3 Turbine Configuration Giving Best Mean Efficiency

The mean total-static efficiencies of the four basic turbines for three speed ratios and for losses determined by two correlations are shown in Fig. 11. Curves have been drawn through the mean efficiencies of each turbine for each loss correlation. Due to the fact that only three points were available for each curve, then the curves have been simplified to arcs of circles. The two individual mean efficiency curves for each particular turbine have been averaged as shown in order to obtain additional curves that correspond to an average mean efficiency. If it is assumed that the averaged mean efficiencies are the mean efficiencies that could reasonably be expected in practice, then some tentative conclusions can be drawn. Before this is done, however, it is convenient to compile the following list (approximate values only).

	Maximum averaged mean efficiency %	Speed corresponding to maximum averaged mean efficiency expressed as a percentage of design speed %
Build 1	74·7	100·8
Build 2	70·1	97·5
Build 3	75·6	100·0
Build 4	70·7	115·8

Clearly the performance of Build 3 is superior to that of the other turbines for the entire speed range considered and this turbine would be the best to use for the pulsating flow considered in this investigation. The performance of Build 1 is always better than that of Builds 2 and 4. Although the best performance of Build 4 is better than the best performance of Build 2, the choice between these two turbines depends upon the speed range considered. At low speeds Build 2 is preferable to Build 4 while at high speeds the converse is true.

An analysis of Fig. 7, which depicts the steady-flow efficiency-velocity ratio curves for the four turbines, indicates that Builds 1 and 2, with outlet blade angles of 60° and 50° respectively, produce the best total-total efficiencies and Builds 1 and 3, with outlet blade angles of 60° and 70° respectively, produce the best total-static efficiencies. This suggests that a turbine with outlet

blade angles in the range 50° to 60° in the first stage and outlet blade angles in the range 60° to 70° in the second stage would give the best total-static efficiencies under steady-flow conditions and better mean total-static efficiencies under pulsating-flow conditions than the four turbines investigated.

5.2.4 Redistribution of Flow Angles by Area Changes

An analysis of Fig. 10, which depicts the manner in which the internal flow characteristics vary throughout Build 1 when it is operating at its design speed, indicates that the incidence angles on the second rotor vary more than those on the first, and are biased toward the negative side over most of the cycle. Also, the second stage does the most work early in the cycle but does the least work later. Consequently, any change of the second rotor inlet angle in the negative direction to give a better average alignment to the flow could be detrimental in the early part of the cycle, when the turbine is highly loaded, but to advantage over the rest of the cycle.

An attempt to obtain improved mean efficiencies was made by changing the flow areas throughout the turbine thereby redistributing the flow directions. The details of the different versions of Build 1 analysed in this investigation are given in Section 3.1.4. This method of altering the matching between the gas flow angles and the inlet blade angles is not as desirable as modifying the inlet blade angles, but the method was relatively simple and involved only minor changes to the efficiency-prediction programme (referred to in Section 3.2).

It was found that a reduction of the second stage flow areas made the second rotor incidence angles more positive but the first rotor incidence angles more negative, with a small net loss in mean total-total efficiency, and a marked decrease in mean total-static efficiency because of the increased exit kinetic energy loss. Conversely, it was found that an increase of the second stage flow areas decreased the mean total-total efficiency but increased the mean total-static efficiency as a result of the reduced exit kinetic energy loss associated with reduced stage loading. Both results are clearly indicated in Fig. 12.

The above attempt to obtain improved mean efficiencies was inconclusive since changes in first rotor incidence angles and second stage exit kinetic energy masked any beneficial effect of incidence angle change on the second rotor: only by specifically varying the second rotor inlet blade angles could the true effect be estimated.

5.3 Comparison of Estimated Mean Efficiencies of Axial Turbines with Estimated Mean Efficiency of Radial Turbine

The present study with axial-flow turbines is an extension of the investigation performed on the radial-inflow turbine (Erm (1973)) to determine the best turbine configuration for operation with the pulsating flow from an experimental combustor. Consequently, it is appropriate to compare the results obtained for the two types of turbine.

The estimated mean efficiencies of the two-stage axial-flow turbines considered in this investigation are listed in Section 5.2.3. Build 3, which has a maximum mean total-static efficiency of about 75·6%, gives the best results. The corresponding maximum mean total-static efficiency of the radial-inflow turbine is about 76·3%. Thus the two types of turbine have much the same efficiency. It is to be noted, however, that a number of other factors have to be considered before any firm conclusions can be drawn on the relative merits of the different turbines.

Although the general form of the pulsating flow used in both investigations is the same (blowdown with uniform combustor conditions and scavenging in which the incoming scavenging air intermixed completely with the undischarged combustor contents), and although an attempt was made to maintain a comparable severity of pulsation (refer to Section 4), the two types of pulsating flow are in actual fact different due to the fact that the temperatures and pressures at the important cycle locations are not the same in both cases.

A factor that must be considered when comparing the performance of the axial-flow turbines with that of the radial-flow type is the relative sizes of the two different types of machine. The capacities of the axial-flow types are smaller than that of the radial-flow type, so the axial-flow turbines may have in fact suffered some penalty as a consequence.

Another factor that must be considered when comparing the performance of the two types of turbine is that no diffuser was incorporated in the axial-flow turbine study whereas one was

used with the radial machine. Consequently, absolute values of mean efficiency for the two types are not directly comparable.

The choice between a two-stage axial-flow turbine and a single-stage radial-inflow turbine will clearly not be decided on turbine efficiency alone. Since the performance is much the same, it is likely that reliability, maintenance needs and cost may be more decisive factors; these factors are all generally improved by simplicity of construction.

6. CONCLUSIONS

An endeavour has been made to estimate the mean efficiencies of a number of different two-stage axial-flow turbines under pulsating-flow operating conditions. Initially the turbine loss characteristics were determined by using the revised Ainley and Mathieson correlation but it was soon found that this correlation was inadequate at high negative angles of incidence and consequently some modification was needed to the correlation in this area of operation. It became quite clear that a better knowledge of turbine loss characteristics at high negative angles of incidence will be needed before more precise optimisation of turbine geometry for operation under pulsating flow can be attempted.

The maximum mean total-static efficiencies that could reasonably be expected in practice from the four basic turbine configurations under pulsating-flow operation are listed below.

Build 1	74·7%
Build 2	70·1%
Build 3	75·6%
Build 4	70·7%

A turbine with outlet blade angles in the range 50° to 60° in the first stage and outlet blade angles in the range 60° to 70° in the second stage could possibly give better mean total-static efficiencies under pulsating-flow conditions than the four turbines investigated.

An analysis of the flow through a turbine during a pulse has shown that the mean inlet flow angles encountered by the different blade rows varies and it may be possible to obtain improved values of mean efficiency if the matching between the inlet flow angles and the inlet blade angles throughout the turbines is improved. An attempt to show this was inconclusive.

Since the indicated performances of a single-stage radial-inflow turbine and a two-stage axial-flow turbine for operation with the assumed pulsating-flow conditions are much the same, then the choice between these two types of turbine will be governed by factors such as simplicity of construction and cost of the engine rather than by performance.

7. ACKNOWLEDGEMENTS

The author wishes to acknowledge gratefully the valuable contributions of Mr. J. E. Williams, who supervised the study and provided guidance, many helpful suggestions and continued support and also to Mr. D. A. Frith, who provided valuable contributions and much assistance during the preparation of this report.

REFERENCES

Ainley, D. G., and Mathieson, G. C. R. — "A Method of Performance Estimation for Axial-Flow Turbines." Aeronautical Research Council, R & M 2974, 1951.

Dunham, J., and Came, P. M. — "Improvements to the Ainley-Matheison Method of Turbine Performance Prediction." Trans. Am. Soc. Mech. Engrs., Jour. of Eng. for Power, Vol. 92, Series A, No. 3, pp. 252–256, July 1970.

Dunham, J., and Panton, J. — "Experiments on the Design of a Small Axial Turbine." Institution of Mechanical Engineers, Conference Publication 3, pp. 56–65, 1973.

Emmert, H. D. — "Current Design Practices for Gas-Turbine Power Elements." Trans. Am. Soc. Mech. Engrs., Vol. 72, pp. 189–200, February 1950.

Erm, L. P. — "Estimation of the Performance of a Typical Radial Turbine Under Conditions of Pulsating Flow." ARL/ME Report 140, March 1973.

Hawthorne, W. R. — "Elements of Turbine and Compressor Theory." Gas Turbine Laboratory Note, Massachusetts Institute of Technology, Unpublished, 1957.

Horlock, J. H. — "Losses and Efficiencies in Axial-Flow Turbines." Int. Jour. Mech. Sci., Vol. 2, pp. 48–75, 1960.

Horlock, J. H. — "Axial Flow Turbines." Butterworth & Co. (Publishers) Ltd., London, 1966.

Horlock, J. H. — "Unsteady Flow in Turbomachines." Institution of Engineers, Australia, Third Australasian Conference on Hydraulics and Fluid Mechanics, Sydney, 1968.

Kroon, R. P., and Tobiasz, H. J. — "Off-Design Performance of Multistage Turbines." Trans. Am. Soc. Mech. Engrs., Jour. of Eng. for Power, Vol. 93, Series A, No. 1, pp. 21–27, January 1971.

Panton, J. — "Small Axial Turbine." Ricardo and Co. Engineers (1927) Ltd., Report No. DP. 10367, October 1967.

Shaw, R. — "Calculations of Turbine Efficiency." University of Liverpool, Department of Mechanical Engineering, Report ULME B7, 1964.

Smith, D. J. L., and Johnston, I. H. — "Investigations on an Experimental Single-Stage Turbine of Conservative Design." "Part I—A Rational Aerodynamic Design Procedure." Aeronautical Research Council, R & M 3541, 1967.

Soderberg, C. R. — Gas Turbine Laboratory, Massachusetts Institute of Technology, Unpublished, 1949.

Williams, J. E. — "The Constant-Volume Gas Turbine—Revision of the Simplified Theoretical Analysis." ARL/ME Note 356, February 1975.

APPENDIX I

PRINCIPAL NOTATION

A	flow area measured normal to camber line. m^2
A_A	annulus area. m^2
A_N	flow area measured normal to flow direction. m^2
a	acoustic velocity. m/s
c	blade chord. m
C_p	specific heat at constant pressure. J/kg.K
h	annulus height. m
i	incidence angle of flow on to a blade row given by difference between gas flow angle relative to blade inlet and blade inlet angle. rad
i_s	stalling incidence angle. rad
k	radial tip clearance. m
M	Mach number.
m_0	mass of gas in combustor. kg
$\dot{m}$	mass flow rate. kg/s
$\dot{m}_{OUT}$	mass flow rate of gas out of combustor. kg/s
Δm_{IN}	increment of mass flowing into combustor. kg
Δm_{OUT}	increment of mass flowing out of combustor. kg
P	total or stagnation pressure. Pa
p	static pressure. Pa
P_{SCAV}	pressure of scavenging air at entry to combustor. Pa
PR_{T1T7}	turbine or stage pressure ratio based upon total pressure at station 1 and total pressure at station 7.
PR_{T7S13}	stage pressure ratio based upon total pressure at station 7 and static pressure at station 13.
PR_{T7T13}	stage pressure ratio based upon total pressure at station 7 and total pressure at station 13.
PR_{T1S13}	turbine pressure ratio based upon total pressure at station 1 and static pressure at station 13.
R	gas constant. J/kg.K
s	blade pitch. m
T	total or stagnation temperature. K
t	static temperature. K
T_{SCAV}	temperature of scavenging air at entry to combustor. K

$\bar{T}_{1(\mathrm{MASS})}$	mean combustor cycle temperature computed on a mass-averaged basis. K
$\bar{T}_{1(\mathrm{TIME})}$	mean combustor cycle temperature computed on a time-averaged basis. K
t_e	blade trailing edge thickness measured normal to camber line at trailing edge. m
t_{max}	maximum blade thickness. m
Δt	time increment. s
U	rotor-blade speed at mean diameter. m/s
V	gas velocity. m/s
V_{ST1S7}	spouting velocity based upon total pressure at station 1 and static pressure at station 7. m/s
v_0	volume of combustor. m^3
W	specific shaft work. J/kg
ΔW_{ACT}	actual increment of work resulting from flow of an increment of mass through turbine. J
ΔW_{IS}	isentropic or theoretical increment of work resulting from flow of an increment of mass through turbine. J
Y_P	profile loss coefficient.
Y_S	secondary loss coefficient.
Y_K	tip clearance loss coefficient.
Y_T	total loss coefficient.

Greck Letters

α	gas flow angle measured relative to axial direction. rad
β	blade angle measured relative to axial direction. rad
γ	specific heat ratio.
η_{T1S7}	turbine or stage efficiency based upon total pressure at station 1 and static pressure at station 7.
η_{T1T7}	turbine or stage efficiency based upon total pressure at station 1 and total pressure at station 7.
η_{T7T13}	stage efficiency based upon total pressure at station 7 and total pressure at station 13.
η_{T1S13}	turbine efficiency based upon total pressure at station 1 and static pressure at station 13.
η_{T1T13}	turbine efficiency based upon total pressure at station 1 and total pressure at station 13.
η_{T1S13}	mean turbine efficiency for cyclic pulsating-flow operating conditions based upon total pressure at station 1 and static pressure at station 13.
η_{T1T13}	mean turbine efficiency for cyclic pulsating-flow operating conditions based upon total pressure at station 1 and total pressure at station 13.
ν_{T1S7}	velocity ratio based upon total pressure at station 1 and static pressure at station 7.
ν_{T1S13}	velocity ratio based upon total pressure at station 1 and static pressure at station 13.

ν_{T1T13} velocity ratio based upon total pressure at station 1 and total pressure at station 13.

Ψ stage loading coefficient ($\Psi = \Delta W/U^2$).

Subscripts

0 station within the combustor.

1 station at first stator inlet.

2 station at first stator throat.

3 station downstream of first stator.

4 station at first rotor inlet.

5 station at first rotor throat.

6 station downstream of first rotor.

7 station at second stator inlet.

8 station at second stator throat.

9 station downstream of second stator.

10 station at second rotor inlet.

11 station at second rotor throat.

12 station downstream of second rotor.

13 station downstream of turbine.

V, W locations on pulsed combustor cycle (see Fig. 8).

APPENDIX II

A2. CALCULATION OF TURBINE LOSS CHARACTERISTICS

The technique used to calculate the turbine loss characteristics by means of the revised Ainley correlation is now described. The analysis is presented for blade row 456 of the turbine under investigation (refer to Fig. 1) but is applicable to any arbitrary blade row provided that the correct geometrical dimensions are used and the subscripts are modified appropriately. It is also to be noted that the following analysis is presented for subsonic flow conditions except where otherwise indicated.

A2.1 *Profile Losses*

The profile loss coefficient at zero incidence can be determined by means of the relationship

$$Y_{P46(0)} = \left[Y_{P(0)\ (\beta_4 = 0)} + \left\{\frac{\beta_4}{\alpha_5}\right\}^2 \left\{ Y_{P(0)\ (\beta_4 = -\alpha_5)} - Y_{P(0)\ (\beta_4 = 0)} \right\} \right] \left\{\frac{t/c}{0{\cdot}2}\right\}^{-\frac{\beta_4}{\alpha_5}} \qquad \text{(A2.1)}$$

In this equation, $Y_{P(0)\ (\beta_4 = 0)}$ is the profile loss coefficient at zero incidence for a blade having $\beta_4 = 0°$ and same α_5 and s/c as the actual blade. $Y_{P(0)\ (\beta_4 = -\alpha_5)}$ is the profile loss coefficient at zero incidence for a blade having $\beta_4 = -\alpha_5$ and same α_5 and s/c as the actual blade. The values of $Y_{P(0)\ (\beta_4 = 0)}$ and $Y_{P(0)\ (\beta_4 = -\alpha_5)}$ can be determined from graphs given by Ainley and Mathieson (1951).

In order to determine the profile loss coefficient for a particular angle of incidence, i, it is first necessary to determine the stalling incidence angle, i_s, from graphs given by Ainley and Mathieson (1951) and then, after computing i/i_s, determine $Y_{P46}/Y_{P46(0)}$ from another graph given in the same reference. Once $Y_{P46}/Y_{P46(0)}$ has been determined then it is a simple matter to calculate Y_{P46}.

For supersonic flow conditions only, it is necessary to use an additional term, viz. $[1 + 60(M_6 - 1)^2]$, when determining profile losses. This term has not been used in the current investigation since all flow conditions considered have been subsonic.

A2.2 *Secondary Losses*

The secondary loss coefficient for any specified angle of incidence can be determined by means of the relationship

$$Y_{S46} = 0{\cdot}0334 \left[\frac{c}{h}\right] \left[\frac{\cos \alpha_5}{\cos \beta_4}\right] \left[\frac{C_L}{s/c}\right]^2 \left[\frac{\cos^2 \alpha_5}{\cos^3 \alpha_{M45}}\right] \qquad \text{(A2.2)}$$

where

$$\frac{C_L}{s/c} = 2 (\tan \alpha_4 - \tan \alpha_5) \cos \alpha_{M45} \qquad \text{(A2.3)}$$

and

$$\tan \alpha_{M45} = 0{\cdot}5 (\tan \alpha_4 + \tan \alpha_5) \qquad \text{(A2.4)}$$

A2.3 *Tip Clearance Losses*

The tip clearance loss coefficient for any specified angle of incidence can be determined by means of the relationship

$$Y_{K46} = B \left[\frac{c}{h}\right] \left\{\frac{k}{c}\right\}^{0{\cdot}78} \left[\frac{C_L}{s/c}\right]^2 \left[\frac{\cos^2 \alpha_5}{\cos^3 \alpha_{M45}}\right] \qquad \text{(A2.5)}$$

The value of B is 0·47 for unshrouded blades while $\frac{C_L}{s/c}$ and α_{M45} can be determined from equations (A2.3) and (A2.4) respectively.

A2.4 *Total Losses*

The total loss coefficient for any specified angle of incidence can be determined by simply adding together the component loss coefficients for this angle of incidence as follows:

$$Y_{T46} = Y_{P46} + Y_{S46} + Y_{K46} \tag{A2.6}$$

The variation of the component loss coefficients, Y_{P46}, Y_{S46} and Y_{K46}, as well as the total loss coefficient, Y_{T46}, with incidence angle, i, for blade row 456 is shown in Fig. 4. Also shown on this figure are the corresponding loss coefficients for blade row 123 for zero incidence angle.

APPENDIX III

A3. THERMODYNAMIC ANALYSIS OF FLOW THROUGH TURBINE AND PREDICTION OF TURBINE EFFICIENCY

The details of the equations used and the technique adopted in order to establish the flow conditions through the turbine to enable the efficiency to be predicted are now described.

A3.1 *Known Data Used in Analysis*

The known data used in the analysis are listed in a number of different groups as follows.

A3.1.1 *Specified Turbine Operating Conditions*

The specified turbine operating conditions are listed below.

T_1	K
P_1	Pa
p_7	Pa
U	m/s

A3.1.2 *Known Thermodynamic Data*

The known thermodynamic data are listed below. It is assumed that the specific heats and other gas constants do not vary with temperature.

$C_p = 1{\cdot}00$ kJ/kg.K
$R = 0{\cdot}287$ kJ/kg.K
$\gamma = 1{\cdot}4$

A3.1.3 *Known Turbine Geometrical Data*

The known turbine geometrical data are listed below.

$A_2 = 1529$ mm^2
$A_{A3} = 3057$ mm^2
$A_5 = 1822$ mm^2
$A_{A6} = 3644$ mm^2
$\beta_2 = -60°$ (Nominal)
$\beta_5 = -60°$ (Nominal)

It should be noted that Ainley and Mathieson (1951) give a method of calculating the gas outlet angle as a function of blade geometrical characteristics and flow Mach number. Since it is shown that for straight-backed blades and $M > 0{\cdot}5$ the actual gas outlet angle does not vary more than a few degrees, it was decided to ignore this variation for the purpose of the present study. Thus a blade design is assumed which will give the nominated gas outlet angle at the higher Mach numbers, and no variation of gas outlet angle with conditions is allowed for. Revision of the method to include gas outlet angle deviation with flow conditions could be incorporated for greater accuracy, provided the accuracy of other data (loss coefficients, etc.) is good enough to warrant this improvement.

A3.2 *Details of Equations Used to Establish Flow Conditions Through Turbine*

As has been stated in Section 2.2, in order to establish the flow conditions through the turbine for the chosen operating conditions it is necessary to adopt an iterative approach. This process involves systematically choosing a series of trial values of p_3 and evaluating tentative

values of the flow variables through the turbine until the mass flow rates through the stator and rotor agree within defined limits.

It is necessary to use alternative sets of equations to evaluate the flow variables through the turbine depending upon whether or not the flow is subsonic or supersonic. Both sets of equations are considered in the following.

A3.2.1 *Analysis of Flow Through Stator*

The analysis of the flow through the stator is subdivided into a number of different sections each of which is an analysis of the flow at a particular stator station for either subsonic or supersonic flow conditions downstream of the stator.

A3.2.1.1 *Subsonic, sonic or supersonic flow downstream of stator (any M_3)*

The following equations, viz. (A3.1) to (A3.7), used to determine flow variables are applicable for any type of flow downstream of the stator.

Station 3: *Downstream of stator*

The total temperature is given by the following relationship:

$$T_3 = T_1 \tag{A3.1}$$

The total loss coefficient for the stator is

$$Y_{T13} = \frac{P_1 - P_3}{P_3 - p_3} \tag{A3.2}$$

This relationship can be transposed to yield the following expression for the total pressure:

$$P_3 = \frac{P_1 + Y_{T13}\, p_3}{1 + Y_{T13}} \tag{A3.3}$$

Now that T_3, P_3 and p_3 are all known, it is possible to determine the static temperature by means of the isentropic relationship

$$t_3 = T_3 \left\{\frac{p_3}{P_3}\right\}^{\frac{\gamma-1}{\gamma}} \tag{A3.4}$$

It is now also possible to determine the absolute gas velocity as follows:

$$V_3 = \sqrt{[2C_p(T_3 - t_3)]} \tag{A3.5}$$

while the acoustic velocity is

$$a_3 = \sqrt{[\gamma R t_3]} \tag{A3.6}$$

so yielding the Mach number

$$M_3 = \frac{V_3}{a_3} \tag{A3.7}$$

If $M_3 < 1{\cdot}0$ then the flow at the throat is subsonic while if $M_3 \geqslant 1{\cdot}0$ then the flow at the throat is sonic. The equations applicable to both of these flow conditions are considered in turn.

A3.2.1.2 *Subsonic flow downstream of stator ($M_3 < 1{\cdot}0$)*

The following equations, viz. (A3.8) to (A3.18), used to determine flow variables are applicable when the flow downstream of the stator is subsonic. For this flow, conditions at stations 2 and 3 are essentially the same.

Station 2: *Stator throat*

Flow variables at the stator throat are given by the following relationships:

$$T_2 = T_1 \tag{A3.8}$$
$$t_2 = t_3 \tag{A3.9}$$
$$P_2 = P_3 \tag{A3.10}$$
$$p_2 = p_3 \tag{A3.11}$$
$$V_2 = V_3 \tag{A3.12}$$
$$a_2 = a_3 \tag{A3.13}$$

$$M_2 = M_3 \tag{A3.14}$$

$$\alpha_2 = \beta_2 \tag{A3.15}$$

The mass flow rate can be determined as follows:

$$\dot{m}_2 = \frac{p_2 A_2 V_2}{R t_2} \tag{A3.16}$$

Station 3: *Downstream of stator*

Flow variables downstream of the stator are given by the following relationships:

$$\dot{m}_3 = \dot{m}_2 \tag{A3.17}$$

$$\alpha_3 = \alpha_2 \tag{A3.18}$$

A3.2.1.3 *Sonic or supersonic flow downstream of stator* ($M_3 \geqslant 1{\cdot}0$)

The following equations, viz. (A3.19) to (A3.29), used to determine flow variables are applicable when the flow downstream of the stator is sonic or supersonic. For supersonic flow, conditions at stations 2 and 3 are different as a consequence of a Prandtl-Meyer expansion between these stations.

Station 2: *Stator throat*

Flow variables at the stator throat are given by the following relationships:

$$T_2 = T_1 \tag{A3.19}$$

$$P_2 = P_3 \tag{A3.20}$$

$$\alpha_2 = \beta_2 \tag{A3.21}$$

A relationship between the total temperature and static temperature is

$$\frac{T}{t} = \left[1 + \frac{(\gamma - 1)}{2} M^2\right] \tag{A3.22}$$

Since the velocity at the stator throat is sonic ($M_2 = 1{\cdot}0$), then the equation for the static temperature is

$$t_2 = \frac{T_2}{\left[1 + \frac{(\gamma - 1)}{2}\right]} \tag{A3.23}$$

A corresponding equation for the static pressure is

$$p_2 = \frac{P_2}{\left[1 + \frac{(\gamma - 1)}{2}\right]^{\frac{\gamma}{\gamma - 1}}} \tag{A3.24}$$

The absolute gas velocity can be determined from the relationship

$$V_2 = \sqrt{[2C_p(T_2 - t_2)]} \tag{A3.25}$$

The mass flow rate can now be determined from

$$\dot{m}_2 = \frac{p_2 A_2 V_2}{R t_2} \tag{A3.26}$$

Station 3: *Downstream of stator*

The mass flow rate is given by the following relationship:

$$\dot{m}_3 = \dot{m}_2 \tag{A3.27}$$

Now, the mass flow rate can be related to flow conditions as follows:

$$\dot{m}_3 = \frac{p_3 A_{A3} V_3 \cos \alpha_3}{R t_3} \tag{A3.28}$$

This expression can be transposed to yield

$$\alpha_3 = \pm \arccos\left[\frac{\dot{m}_3 R t_3}{p_3 A_{A3} V_3}\right] \tag{A3.29}$$

where t_3 and V_3 are given by equations (A3.4) and (A3.5) respectively.

In accordance with the sign convention adopted for gas flow angles, the sign of α_3 can be determined as follows:

$$\begin{aligned} &\text{if } \alpha_2 > 0 \quad \text{then} \quad \alpha_3 > 0 \\ &\text{if } \alpha_2 \leqslant 0 \quad \text{then} \quad \alpha_3 \leqslant 0 \end{aligned}$$

A3.2.2 *Analysis of Flow at Rotor Inlet*

The following equations, viz. (A3.30) to (A3.40), used to determine flow variables at the rotor inlet are applicable regardless of Mach number downstream of the stator. The subscripts 4, 5 and 6 on flow variables indicate that these variables are specified relative to the rotor.

Flow variables at the rotor inlet are given by the following relationships:

$$t_4 = t_3 \tag{A3.30}$$
$$p_4 = p_3 \tag{A3.31}$$
$$\dot{m}_4 = \dot{m}_3 \tag{A3.32}$$
$$a_4 = a_3 \tag{A3.33}$$

With reference to Fig. 1 it is apparent that

$$V_3 \cos \alpha_3 = V_4 \cos \alpha_4 \tag{A3.34}$$

and, having regard for the sign convention,

$$V_3 \sin \alpha_3 - U = -V_4 \sin \alpha_4 \tag{A3.35}$$

so therefore

$$\alpha_4 = -\operatorname{artan}\left[\frac{V_3 \sin \alpha_3 - U}{V_3 \cos \alpha_3}\right] \tag{A3.36}$$

and

$$V_4 = \frac{V_3 \cos \alpha_3}{\cos \alpha_4} \tag{A3.37}$$

The total temperature can be determined from the relationship

$$T_4 = t_4 + \frac{V_4^2}{2C_p} \tag{A3.38}$$

The total pressure is given by the isentropic relationship

$$P_4 = p_4 \left\{\frac{T_4}{t_4}\right\}^{\frac{\gamma}{\gamma-1}} \tag{A3.39}$$

The Mach number can be determined as follows:

$$M_4 = \frac{V_4}{a_4} \tag{A3.40}$$

A3.2.3 *Analysis of Flow Through Rotor*

The analysis of the flow through the rotor is subdivided into a number of different sections each of which is an analysis of the flow at a particular rotor station for either subsonic or supersonic flow conditions downstream of the rotor.

Since the analysis of the flow through the rotor is very similar to the analysis considered earlier for the stator, in order to simplify the presentation, the equations used to determine flow variables will often just be listed without the accompanying text and intermediate steps.

A3.2.3.1 *Subsonic, sonic or supersonic flow downstream of rotor (any M_6)*

The following equations, viz. (A3.41) to (A3.47), used to determine flow variables are applicable for any type of flow downstream of the rotor.

Station 6: *Downstream of rotor*

Flow variables downstream of the rotor are given by the following relationships:

$$T_6 = T_4 \tag{A3.41}$$

$$p_6 = p_7 \tag{A3.42}$$

where p_7 is a specified turbine operating condition.

Other flow variables downstream of the rotor can be determined as follows:

$$P_6 = \frac{P_4 + Y_{T46}\, p_6}{1 + Y_{T46}} \tag{A3.43}$$

where Y_{T46} is a function of the incidence angle, i_4

$$t_6 = T_6 \left\{\frac{p_6}{P_6}\right\}^{\frac{\gamma-1}{\gamma}} \tag{A3.44}$$

$$V_6 = \sqrt{[2C_p(T_6 - t_6)]} \tag{A3.45}$$

$$a_6 = \sqrt{[\gamma R t_6]} \tag{A3.46}$$

$$M_6 = \frac{V_6}{a_6} \tag{A3.47}$$

If $M_6 < 1{\cdot}0$ then the flow at the throat is subsonic while if $M_6 \geqslant 1{\cdot}0$ then it is sonic. The equations applicable to both of these flow conditions shall be considered in turn.

A3.2.3.2 *Subsonic flow downstream of rotor* ($M_6 < 1{\cdot}0$)

The following equations, viz. (A3.48) to (A3.58), used to determine flow variables are applicable when the flow downstream of the rotor is subsonic. For this flow, conditions at stations 5 and 6 are essentially the same.

Station 5: *Rotor throat*

Flow variables at the rotor throat are given by the following relationships:

$$T_5 = T_4 \tag{A3.48}$$

$$t_5 = t_6 \tag{A3.49}$$

$$P_5 = P_6 \tag{A3.50}$$

$$p_5 = p_6 \tag{A3.51}$$

$$V_5 = V_6 \tag{A3.52}$$

$$a_5 = a_6 \tag{A3.53}$$

$$M_5 = M_6 \tag{A3.54}$$

$$\alpha_5 = \beta_5 \tag{A3.55}$$

The mass flow rate can be determined by means of the relationship

$$\dot{m}_5 = \frac{p_5 A_5 V_5}{R t_5} \tag{A3.56}$$

Station 6: *Downstream of rotor*

Flow variables downstream of the rotor are given by the following relationships:

$$\dot{m}_6 = \dot{m}_5 \tag{A3.57}$$

$$\alpha_6 = \alpha_5 \tag{A3.58}$$

A3.2.3.3 *Sonic and supersonic flow downstream of rotor* ($M_6 \geqslant 1{\cdot}0$)

The following equations, viz. (A3.59) to (A3.67), used to determine flow variables are applicable when the flow downstream of the rotor is sonic or supersonic.

Station 5: *Rotor throat*

Flow variables at the rotor throat are given by the following relationships:

$$T_5 = T_4 \tag{A3.59}$$

$$P_5 = P_6 \tag{A3.60}$$

$$\alpha_5 = \beta_5 \tag{A3.61}$$

Other flow variables at the rotor throat can be determined by means of the relationships shown below:

$$t_5 = \frac{T_5}{\left[1 + \frac{(\gamma-1)}{2}\right]} \tag{A3.62}$$

$$p_5 = \frac{P_5}{\left[1 + \frac{(\gamma-1)}{2}\right]^{\frac{\gamma}{\gamma-1}}} \tag{A3.63}$$

$$V_5 = \sqrt{[2C_p(T_5 - t_5)]} \tag{A3.64}$$

$$\dot{m}_5 = \frac{p_5 A_5 V_5}{R t_5} \tag{A3.65}$$

Station 6: *Downstream of rotor*

The mass flow rate is given by the following relationship:

$$\dot{m}_6 = \dot{m}_5 \tag{A3.66}$$

The gas flow angle can be determined by means of the relationship shown below:

$$\alpha_6 = \pm \arccos\left[\frac{\dot{m}_6 R t_6}{p_6 A_{A6} V_6}\right] \tag{A3.67}$$

where t_6 and V_6 are given by equations (A3.44) and (A3.45) respectively.

In accordance with the sign convention adopted for gas flow angles, the sign of α_6 can be determined as follows:

$$\text{if } \alpha_5 > 0 \quad \text{then} \quad \alpha_6 > 0$$

$$\text{if } \alpha_5 \leqslant 0 \quad \text{then} \quad \alpha_6 \leqslant 0$$

A3.2.4 *Analysis of Flow at a Fixed Station Downstream of Rotor*

Since the analysis of the flow at a fixed station downstream of the rotor is very similar to the analysis considered earlier for the rotor inlet, then in order to simplify the presentation, the equations used to determine flow variables will often just be listed without the accompanying text and intermediate steps.

The following equations, viz. (A3.68) to (A3.75), used to determine flow variables at a fixed station downstream of the rotor are applicable regardless of Mach number downstream of the rotor.

$$t_7 = t_6 \tag{A3.68}$$

$$\dot{m}_7 = \dot{m}_6 \tag{A3.69}$$

$$a_7 = a_6 \tag{A3.70}$$

$$\alpha_7 = -\operatorname{artan}\left[\frac{V_6 \sin\alpha_6 - U}{V_6 \cos\alpha_6}\right] \tag{A3.71}$$

$$V_7 = \frac{V_6 \cos\alpha_6}{\cos\alpha_7} \tag{A3.72}$$

$$T_7 = t_7 + \frac{V_7^2}{2C_p} \tag{A3.73}$$

$$P_7 = p_7 \left\{\frac{T_7}{t_7}\right\}^{\frac{\gamma}{\gamma-1}} \tag{A3.74}$$

$$M_7 = \frac{V_7}{a_7} \tag{A3.75}$$

A3.3 *Balancing of Mass Flow Rates*

As has been indicated in Section A3.2 in order to establish the flow conditions through the turbine for the chosen operating conditions it is necessary to adopt an iterative approach. This process involves systematically choosing a series of trial values of p_s and evaluating the flow variables through the turbine until the mass flow rates through the stator and rotor, as determined by equations (A3.16) or (A3.26) (stator) and (A3.56) or (A3.65) (rotor), agree within defined limits.

A3.4 *Prediction of Turbine Efficiency*

As soon as the flow conditions through the turbine have been firmly established for the chosen operating conditions it is possible to determine the total-static efficiency and the velocity ratio as well as the specific work.

The total-static efficiency can be determined as follows:

$$\eta_{T1S7} = \frac{T_1 - T_7}{T_1\left[1 - \left\{\frac{p_7}{P_1}\right\}^{\frac{\gamma-1}{\gamma}}\right]} \tag{A3.76}$$

The velocity ratio is given by

$$\nu_{T1S7} = \frac{U}{V_{ST1S7}} \tag{A3.77}$$

where V_{ST1S7} is the spouting velocity which is defined as that velocity which has an associated kinetic energy equal to the isentropic enthalpy drop across the turbine. If V_{ST1S7} is expressed in terms of thermodynamic variables, the velocity ratio becomes

$$\nu_{T1S7} = \frac{U}{\sqrt{\left[2C_pT_1\left(1 - \left\{\frac{p_7}{P_1}\right\}^{\frac{\gamma-1}{\gamma}}\right)\right]}} \tag{A3.78}$$

Finally, the specific work can be determined as follows:

$$W_{17} = C_p\,(T_1 - T_7) \tag{A3.79}$$

APPENDIX IV

A4. ESTIMATION OF TURBINE MEAN EFFICIENCY UNDER PULSATING-FLOW CONDITIONS

The technique used to estimate the mean efficiencies of the two-stage turbines when they are operating under the idealised pulsating-flow conditions outlined in Section 4 and Fig. 8 is now described. In the following analysis static pressures and temperatures are used when dealing with combustor conditions. It is assumed that total pressures and temperatures at the turbine inlet are equal to their respective static values within the combustor. The analysis is simplified by assuming that all flow is one-dimensional and that the specific heats and other gas constants do not vary with temperature.

A4.1 *Blowdown Phase*

During the blowdown phase there is no cold scavenging air flowing into the combustor and the pressure continually decreases as the hot gas in discharged through the turbine.

The analysis of the blowdown phase is described for the first time interval (01), but is applicable to all subsequent intervals.

In order to commence the calculations it is necessary to select a trial value of t_{0v}, the combustor temperature before combustion (see Fig. 8).

The initial mass of gas in the combustor is given by

$$m_0(0) = \frac{p_{0v}\, v_0}{R\, t_{0v}} \tag{A4.1}$$

Instead of computing the true mass flow rates through the different turbines, a simpler approach was adopted whereby pseudo mass flow rates were determined after first assuming that the turbines were replaced by a nozzle, of area A_2, acted upon by the pressure ratio $P_1(0)/p_{13}$. With this simplified approach the relationship between the mass discharged from the combustor, the combustor temperature and pressure (i.e. turbine inlet conditions) and the turbine efficiency, at any instant of the pulsating-flow cycle, is the same as if the true mass flow rates had been used and, consequently, the computed mean efficiencies are the same as those which would be obtained by using the true mass flow rates. For the simplified approach, the critical pressure ratio, i.e. the pressure ratio corresponding to $M_2(0) = 1{\cdot}0$, can be determined as follows:

$$\left\{\frac{P_1}{p_{13}}\right\}_{\text{CRIT}} = \left[1 + \frac{(\gamma - 1)}{2}\right]^{\frac{\gamma}{\gamma-1}} \tag{A4.2}$$

If $$\frac{P_1(0)}{p_{13}} \geqslant \left\{\frac{P_1}{p_{13}}\right\}_{\text{CRIT}}, \quad \text{then}$$

$$M_2(0) = 1{\cdot}0 \tag{A4.3}$$

If $$\frac{P_1(0)}{p_{13}} < \left\{\frac{P_1}{p_{13}}\right\}_{\text{CRIT}}, \quad \text{then}$$

$$M_2(0) = \sqrt{\left[\frac{2}{(\gamma - 1)}\left[\left\{\frac{P_1(0)}{p_{13}}\right\}^{\frac{\gamma-1}{\gamma}} - 1\right]\right]} \tag{A4.4}$$

Now that the value of $M_2(0)$ is known, the pseudo mass flow rate through the turbine (out of the combustor) can be determined as follows:

$$\dot{m}_{OUT}(0) = A_2 M_2(0) P_1(0) \sqrt{\frac{\gamma}{RT_1(0)}} \left[\frac{1}{1 + \frac{(\gamma - 1)}{2} M_2^2(0)} \right]^{\frac{\gamma+1}{2(\gamma-1)}} \tag{A4.5}$$

This rate is assumed to apply for the whole interval, and the increment of outflow for the period is

$$\Delta m_{OUT}(01) = \dot{m}_{OUT}(0).\Delta t(01) \tag{A4.6}$$

The ideal or isentropic increment of work obtainable from the turbine in the interval is therefore

$$\Delta W_{IS}(01) = \Delta m_{OUT}(01).C_p.T_1(0) \left[1 - \left\{ \frac{p_{13}}{P_1(0)} \right\}^{\frac{\gamma-1}{\gamma}} \right] \tag{A4.7}$$

In order to determine the actual increment of work, the initial turbine efficiency, $\eta_{T1S13}(0)$, must be determined. Before this can be done, it is necessary to calculate the initial velocity ratio, $\nu_{T1S13}(0)$, by means of the following relationship:

$$\nu_{T1S13}(0) = \frac{U}{\sqrt{\left[\frac{1}{S} \left[2C_p T_1(0) \left[1 - \left\{ \frac{p_{13}}{P_1(0)} \right\}^{\frac{\gamma-1}{\gamma}} \right] \right] \right]}} \tag{A4.8}$$

where S is the number of stages.

The value of $\eta_{T1S13}(0)$ is determined from the appropriate η_{T1S13} versus ν_{T1S13} relationship shown in Fig. 7. It is now possible to determine the actual increment of work as follows:

$$\Delta W_{ACT}(01) = \Delta W_{IS}(01).\eta_{T1S13}(0) \tag{A4.9}$$

Before the flow through the turbine during time interval (12) can be analysed, the combustor pressure and temperature at the end of interval (01) must be determined. The mass of gas in the combustor at the end of interval (01) is

$$m_0(1) = m_0(0) - \Delta m_{OUT}(01) \tag{A4.10}$$

Assuming that the gas remaining in the combustor expands isentropically during interval (01), the new conditions of pressure and temperature are

$$p_0(1) = p_0(0) \left\{ \frac{m_0(1)}{m_0(0)} \right\}^{\gamma} \tag{A4.11}$$

$$t_0(1) = t_0(0) \left\{ \frac{m_0(1)}{m_0(0)} \right\}^{\gamma-1} \tag{A4.12}$$

These are the initial conditions for time interval (12).

The flow through the turbine during time interval (12) can now be analysed. The procedure used is the same as that outlined above for time interval (01) except that $T_1(0)$ is replaced by $T_1(1)$, and likewise for other variables. This process can be repeated for subsequent time intervals until the combustor pressure is found to be equal to or less than the scavenging pressure, P_{SCAV}. When this occurs the scavenging phase is commenced.

A4.2 *Scavenging Phase*

During the scavenging phase the cold incoming air is assumed to intermix completely with the hot undischarged combustor contents and the pressure in the combustor remains constant.

For the first time interval (IJ) of the scavenging phase, the turbine entry conditions, $T_1(I)$ and $P_1(I)$, are equal to those at the end of blowdown and therefore $\Delta m_{OUT}(IJ)$, $\Delta W_{IS}(IJ)$ and $\Delta W_{ACT}(IJ)$ can be determined by using the same method as that outlined above for the blowdown phase. During the first time interval (IJ) the increment of mass of cold scavenging air flowing into the combustor is given by the following relationship (volume inflow equals volume outflow):

$$\Delta m_{IN}(IJ) = \frac{\Delta m_{OUT}(IJ).\, t_0(I)}{T_{SCAV}} \tag{A4.13}$$

Before the flow through the turbine during time interval (JK) can be analysed, it is necessary to determine the combustor temperature at the end of interval (IJ). An expression for this temperature is now developed.

At the end of time interval (IJ) the combustor contains $[m_0(I) - \Delta m_{OUT}(IJ)]$ kg of hot gas at temperature $t_0(I)$ and $\Delta m_{IN}(IJ)$ kg of cold scavenging air at temperature T_{SCAV}. That is

$$m_0(J) = m_0(I) - \Delta m_{OUT}(IJ) + \Delta m_{IN}(IJ) \tag{A4.14}$$

If the hot gas and the cold air mix completely, then the temperature of the mixture is given by the relationship:

$$t_0(J) = \frac{t_0(I)\,[m_0(I) - \Delta m_{OUT}(IJ)] + T_{SCAV}.\Delta m_{IN}(IJ)}{m_0(J)} \tag{A4.15}$$

This is the initial temperature for time interval (JK).

The flow through the turbine during time interval (JK) can now be analysed. The procedure used is the same at that outlined above for time interval (IJ) except that $T_1(I)$ is replaced by $T_1(J)$ and likewise for other variables. This process can be repeated for subsequent time intervals until scavenging is terminated at the point where the sum of the increments of mass inflow equal the mass capacity of the combustor at scavenging pressure and temperature, that is

$$\sum_{X}^{Y} \Delta m_{IN} = \frac{P_{SCAV}\, v_0}{R\, T_{SCAV}} \tag{A4.16}$$

The combustor temperature, t_0, at the end of the last scavenging time interval can then be compared with the trial value of t_{0v} selected at the start of the blowdown analysis. If there is a large discrepancy between these two values of temperature, then the value of t_{0v} can be modified and the cycle calculations repeated until the agreement is acceptable.

A4.3 *Estimation of a Mean Turbine Efficiency*

The mean efficiency over the whole cycle can be evaluated from

$$\bar{\eta}_{T1S13} = \frac{\sum_{W}^{Y} \Delta W_{ACT}}{\sum_{W}^{Y} \Delta W_{IS}} \tag{A4.17}$$

TABLE I

Details of Blade Characteristics at Reference Diameter for Single-Stage Turbine

Details of Stator Row	
Inlet Blade Angle. β_1	0°
Outlet Blade Angle. β_2 (nominal)	−60°
Inlet Gas Angle. α_1	0°
Outlet Gas Angle. α_2	−60°
Blade Pitch/Blade Chord. s/c	0·75
Maximum Blade Thickness/Blade Chord. t_{max}/c	0·200
Radial Tip Clearance/Annulus Height. k/h	0·010
Annulus Height/Blade Chord. h/c	1·2
Details of Rotor Row	
Inlet Blade Angle. β_4	0°
Outlet Blade Angle. β_5 (nominal)	−60°
Inlet Gas Angle. α_4	Variable
Outlet Gas Angle. α_5	−60°
Blade Pitch/Blade Chord. s/c	0·75
Maximum Blade Thickness/Blade Chord. t_{max}/c	0·200
Radial Tip Clearance/Annulus Height. k/h	0·020
Annulus Height/Blade Chord. h/c	1·2

TABLE II

Design Point Flow Conditions and Flow Areas for Single-Stage Turbine

Station Number	T K	t K	P kPa	p kPa	V m/s	M	α °	β ° (nom.)	A_A mm²	A_N mm²	A mm²
1	600·0	589·9	620·6	584·9	142·3	0·292	0·0	0	2607	2607	2607
2	600·0	559·7	603·7	473·3	284·6	0·600	−60·0	−60	3057	1529	1529
3	600·0	559·7	603·7	473·3	284·6	0·600	−60·0		3057	1529	
4	569·8	559·7	503·7	473·3	142·3	0·300	0·0	0	3057	3057	3057
5	569·8	529·5	485·6	375·7	284·6	0·617	−60·0	−60	3644	1822	1822
6	569·8	529·5	485·6	375·7	284·6	0·617	−60·0		3644	1822	
7	539·6	529·5	401·3	375·7	142·3	0·309	0·0		3644	3644	

$\dot{m} = 1{\cdot}283$ kg/s $\qquad Y_{T13(0)} = 0{\cdot}1296$

$U = 246{\cdot}5$ m/s $\qquad Y_{T46(0)} = 0{\cdot}1647$

TABLE III

Predicted Values of Efficiency Corresponding to Two Methods of Loss Determination for Chosen Operating Conditions

Run	Chosen Operating Conditions				Derived Flow Variables when Turbine Loss Characteristics Determined by Revised Ainley Correlation								Derived Flow Variables when Turbine Rotor Loss Characteristics Determined by $Y_{T46} = 0{\cdot}3231 \tan^2 i_4 + 0{\cdot}1647$							
	T_1 K	P_1 kPa	p_7 kPa	U m/s	$\dot{m}$ kg/s	i_4 °	Y_{T13}	Y_{T46}	ν_{T1S7}	η_{T1S7} %	$\frac{\nu_{T1S7}}{\nu_{OPT}}$	$\frac{\eta_{T1S7}}{\eta_{MAX}}$	$\dot{m}$ kg/s	i_4 °	Y_{T13}	Y_{T46}	ν_{T1S7}	η_{T1S7} %	$\frac{\nu_{T1S7}}{\nu_{OPT}}$	$\frac{\eta_{T1S7}}{\eta_{MAX}}$
1	600·0	620·6	375·7	246·5	1·283	0·00	0·1296	0·1647	0·614	75·41	0·937	0·996	1·283	0·00	0·1296	0·1647	0·614	75·41	1·000	1·000
2	600·0	620·6	375·7	91·4	1·292	47·70	0·1296	0·4386	0·228	46·79	0·348	0·618	1·264	47·05	0·1296	0·5375	0·228	45·21	0·371	0·600
3	600·0	620·6	375·7	121·9	1·283	41·25	0·1296	0·3614	0·304	56·77	0·464	0·750	1·270	40·76	0·1296	0·4048	0·304	55·86	0·495	0·741
4	600·0	620·6	375·7	152·4	1·277	33·21	0·1296	0·2933	0·380	64·43	0·580	0·851	1·275	33·10	0·1296	0·3020	0·380	64·24	0·619	0·852
5	600·0	620·6	375·7	182·9	1·276	23·63	0·1296	0·2384	0·456	70·01	0·696	0·925	1·278	23·79	0·1296	0·2275	0·456	70·29	0·743	0·932
6	600·0	620·6	375·7	213·4	1·277	12·61	0·1296	0·1967	0·532	73·58	0·812	0·972	1·280	12·93	0·1296	0·1817	0·532	74·02	0·866	0·982
7	600·0	620·6	375·7	243·8	1·281	0·99	0·1296	0·1668	0·608	75·35	0·928	0·995	1·281	0·99	0·1296	0·1648	0·608	75·41	0·990	1·000
8	600·0	620·6	375·7	274·3	1·288	−10·18	0·1296	0·1451	0·684	75·54	1·044	0·998	1·281	−11·15	0·1296	0·1772	0·684	74·42	1·114	0·987
9	600·0	620·6	375·7	304·8	1·298	−19·91	0·1296	0·1286	0·760	74·37	1·160	0·982	1·279	−22·64	0·1296	0·2209	0·760	71·02	1·238	0·942
10	600·0	620·6	375·7	335·3	1·311	−27·99	0·1296	0·1154	0·836	71·99	1·276	0·951	1·275	−32·80	0·1296	0·2989	0·836	65·13	1·362	0·864
11	600·0	620·6	375·7	365·8	1·326	−34·48	0·1296	0·1046	0·912	68·51	1·392	0·905	1·270	−41·28	0·1296	0·4138	0·912	56·74	1·485	0·752
12	600·0	620·6	375·7	396·2	1·343	−39·50	0·1296	0·0959	0·988	63·97	1·508	0·845	1·263	−48·20	0·1296	0·5690	0·988	45·81	1·609	0·607
13	600·0	620·6	375·7	426·7	1·361	−43·44	0·1296	0·0890	1·064	58·41	1·624	0·772	1·253	−54·08	0·1296	0·7804	1·064	31·94	1·733	0·424
14	600·0	620·6	375·7	457·2	1·379	−46·62	0·1296	0·0835	1·140	51·89	1·740	0·685	1·239	−59·01	0·1296	1·0600	1·140	14·93	1·857	0·198
15	600·0	620·6	375·7	487·7	1·398	−49·12	0·1296	0·0793	1·216	44·37	1·856	0·586								
16	600·0	620·6	375·7	518·2	1·415	−51·08	0·1296	0·0762	1·292	35·82	1·973	0·473								
17	600·0	620·6	375·7	548·6	1·432	−52·69	0·1296	0·0739	1·368	26·29	2·089	0·347								
18	600·0	620·6	375·7	579·1	1·446	−53·94	0·1296	0·0724	1·444	15·63	2·205	0·206								
19	600·0	620·6	375·7	609·6	1·458	−54·96	0·1296	0·0714	1·520	3·91	2·321	0·052								
					$\eta_{MAX} = 75{\cdot}7\%$ (Determined Graphically) $\nu_{OPT} = 0{\cdot}655$ (Determined Graphically)								$\eta_{MAX} = 75{\cdot}41\%$ (Determined Graphically) $\nu_{OPT} = 0{\cdot}614$ (Determined Graphically)							

TABLE IV

Details of Blade Characteristics at Reference Diameter for Two-Stage Turbines

Blade Geometrical Characteristic	Turbine Build Number			
	1	2	3	4
First Stator				
Inlet Blade Angle. β_1	0	0	0	0
Outlet Blade Angle. β_2 (nominal)	−60	−50	−70	−60
Inlet Gas Angle. α_1	0	0	0	0
Outlet Gas Angle. α_2	−60	−50	−70	−60
Blade Pitch/Blade Chord. s/c	0·75	0·75	0·75	0·75
Maximum Blade Thickness/Blade Chord. t_{max}/c	0·200	0·200	0·200	0·200
Radial Tip Clearance/Annulus Height. k/h	0·010	0·010	0·010	0·010
Annulus Height/Blade Chord. h/c	1·2	1·2	1·2	1·2
First Rotor				
Inlet Blade Angle. β_4	0	0	0	30
Outlet Blade Angle. β_5 (nominal)	−60	−50	−70	−60
Inlet Gas Angle. α_4 (design value)	0	0	0	30
Outlet Gas Angle. α_5	−60	−50	−70	−60
Blade Pitch/Blade Chord. s/c	0·75	0·75	0·75	0·75
Maximum Blade Thickness/Blade Chord. t_{max}/c	0·200	0·200	0·200	0·200
Radial Tip Clearance/Annulus Height. k/h	0·020	0·020	0·020	0·020
Annulus Height/Blade Chord. h/c	1·2	1·2	1·2	1·2
Second Stator				
Inlet Blade Angle. β_7	0	0	0	30
Outlet Blade Angle. β_8 (nominal)	−60	−50	−70	−60
Inlet Gas Angle. α_7 (design value)	0	0	0	30
Outlet Gas Angle. α_8	−60	−50	−70	−60
Blade Pitch/Blade Chord. s/c	0·75	0·75	0·75	0·75
Maximum Blade Thickness/Blade Chord. t_{max}/c	0·200	0·200	0·200	0·200
Radial Tip Clearance/Annulus Height. k/h	0·010	0·010	0·010	0·010
Annulus Height/Blade Chord. h/c	1·2	1·2	1·2	1·2
Second Rotor				
Inlet Blade Angle. β_{10}	0	0	0	30
Outlet Blade Angle. β_{11} (nominal)	−60	−50	−70	−60
Inlet Gas Angle. α_{10} (design value)	0	0	0	30
Outlet Gas Angle. α_{11}	−60	−50	−70	−60
Blade Pitch/Blade Chord. s/c	0·75	0·75	0·75	0·75
Maximum Blade Thickness/Blade Chord. t_{max}/c	0·200	0·200	0·200	0·200
Radial Tip Clearance/Annulus Height. k/h	0·020	0·020	0·020	0·020
Annulus Height/Blade Chord. h/c	1·2	1·2	1·2	1·2

TABLE V

Design Point Flow Conditions and Flow Areas for the Four Two-Stage Turbines

Turbine Build Number 1

Station Number	T K	t K	P kPa	p kPa	V m/s	M	α °	β ° (nom.)	A_A mm²	A_N mm²	A mm²
1	600·0	589·9	620·6	584·9	142·3	0·292	0·0	0	2607	2607	2607
2	600·0	559·7	603·7	473·3	284·6	0·600	−60·0	−60	3057	1529	1529
3	600·0	559·7	603·7	473·3	284·6	0·600	−60·0		3057	1529	
4	569·8	559·7	503·7	473·3	142·3	0·300	0·0	0	3057	3057	3057
5	569·8	529·5	485·6	375·7	284·6	0·617	−60·0	−60	3644	1822	1822
6	569·8	529·5	485·6	375·7	284·6	0·617	−60·0		3644	1822	
7	539·6	529·5	401·3	375·7	142·3	0·309	0·0	0	3644	3644	3644
8	539·6	499·3	389·3	296·7	284·6	0·636	−60·0	−60	4351	2175	2175
9	539·6	499·3	389·3	296·7	284·6	0·636	−60·0		4351	2175	
10	509·3	499·3	318·1	296·7	142·3	0·318	0·0	0	4351	4351	4351
11	509·3	469·1	305·5	229·0	284·6	0·656	−60·0	−60	5296	2648	2648
12	509·3	469·1	305·5	229·0	284·6	0·656	−60·0		5296	2648	
13	479·1	469·1	246·6	229·0	142·3	0·328	0·0		5296	5296	

$\dot{m} = 1{\cdot}283$ kg/s
$U = 246{\cdot}5$ m/s

$Y_{T13(0)} = 0{\cdot}1296$
$Y_{T46(0)} = 0{\cdot}1647$
$Y_{T79(0)} = 0{\cdot}1296$
$Y_{T1012(0)} = 0{\cdot}1647$

Turbine Build Number 2

1	600·0	578·7	620·6	546·9	206·8	0·429	0·0	0	1882	1882	1882
2	600·0	548·5	603·2	440·7	321·7	0·686	−50·0	−50	2214	1423	1423
3	600·0	548·5	603·2	440·7	321·7	0·686	−50·0		2214	1423	
4	569·8	548·5	503·5	440·7	206·8	0·441	0·0	0	2214	2214	2214
5	569·8	518·3	485·6	348·5	321·7	0·706	−50·0	−50	2645	1700	1700
6	569·8	518·3	485·6	348·5	321·7	0·706	−50·0		2645	1700	
7	539·6	518·3	401·2	348·5	206·8	0·453	0·0	0	2645	2645	2645
8	539·6	488·1	388·9	273·8	321·7	0·727	−50·0	−50	3171	2038	2038
9	539·6	488·1	388·9	273·8	321·7	0·727	−50·0		3171	2038	
10	509·3	488·1	317·9	273·8	206·8	0·467	0·0	0	3171	3171	3171
11	509·3	457·8	305·5	210·4	321·7	0·751	−50·0	−50	3871	2489	2489
12	509·3	457·8	305·5	210·4	321·7	0·751	−50·0		3871	2489	
13	479·1	457·8	246·6	210·4	206·8	0·482	0·0		3871	3871	

$\dot{m} = 1{\cdot}283$ kg/s
$U = 246{\cdot}5$ m/s

$Y_{T13(0)} = 0{\cdot}1062$
$Y_{T46(0)} = 0{\cdot}1303$
$Y_{T79(0)} = 0{\cdot}1062$
$Y_{T1012(0)} = 0{\cdot}1303$

TABLE V—continued

Design Point Flow Conditions and Flow Areas for the Four Two-Stage Turbines

Turbine Build Number 3

Station Number	T K	t K	P kPa	p kPa	V m/s	M	α °	β ° (nom.)	A_A mm²	A_N mm²	A mm²
1	600·0	596·0	620·6	606·2	89·7	0·183	0·0	0	4032	4032	4032
2	600·0	565·8	601·6	489·8	262·3	0·550	−70·0	−70	4737	1620	1620
3	600·0	565·8	601·6	489·8	262·3	0·550	−70·0		4737	1620	
4	569·8	565·8	502·1	489·8	89·7	0·188	0·0	0	4737	4737	4737
5	569·8	535·6	481·1	387·4	262·3	0·566	−70·0	−70	5670	1939	1939
6	569·8	535·6	481·1	387·4	262·3	0·566	−70·0		5670	1939	
7	539·6	535·6	397·6	387·4	89·7	0·193	0·0	0	5670	5670	5670
8	539·6	505·3	384·2	305·4	262·3	0·582	−70·0	−70	6785	2321	2321
9	539·6	505·3	384·2	305·4	262·3	0·582	−70·0		6785	2321	
10	509·3	505·3	314·0	305·4	89·7	0·199	0·0	0	6785	6785	6785
11	509·3	475·1	299·6	234·8	262·3	0·601	−70·0	−70	8297	2838	2838
12	509·3	475·1	299·6	234·8	262·3	0·601	−70·0		8297	2838	
13	479·1	475·1	241·9	234·8	89·7	0·205	0·0		8297	8297	

$\dot{m}$ = 1·283 kg/s
U = 246·5 m/s

$Y_{T13(0)}$ = 0·1695
$Y_{T46(0)}$ = 0·2226
$Y_{T79(0)}$ = 0·1695
$Y_{T1012(0)}$ = 0·2226

Turbine Build Number 4

1	600·0	588·7	620·6	580·5	150·9	0·311	0·0	0	2472	2472	2472
2	600·0	554·7	601·8	457·1	301·8	0·640	−60·0	−60	2958	1479	1479
3	600·0	554·7	601·8	457·1	301·8	0·640	−60·0		2958	1479	
4	569·8	554·7	502·2	457·1	174·3	0·369	30·0	30	2958	2561	2561
5	569·8	524·4	469·5	351·3	301·8	0·658	−60·0	−60	3639	1820	1820
6	569·8	524·4	469·5	351·3	301·8	0·658	−60·0		3639	1820	
7	539·6	524·4	388·0	351·3	174·3	0·380	30·0	30	3639	3152	3152
8	539·6	494·2	366·5	269·6	301·8	0·678	−60·0	−60	4469	2234	2234
9	539·6	494·2	366·5	269·6	301·8	0·678	−60·0		4469	2234	
10	509·3	494·2	299·6	269·6	174·3	0·391	30·0	30	4469	3870	3870
11	509·3	464·0	278·2	200·8	301·8	0·700	−60·0	−60	5633	2817	2817
12	509·3	464·0	278·2	200·8	301·8	0·700	−60·0		5633	2817	
13	479·1	464·0	224·6	200·8	174·3	0·404	30·0		5633	4879	

$\dot{m}$ = 1·283 kg/s
U = 174·3 m/s

$Y_{T13(0)}$ = 0·1296
$Y_{T46(0)}$ = 0·2753
$Y_{T79(0)}$ = 0·2209
$Y_{T1012(0)}$ = 0·2753

TABLE VI

Efficiency-Velocity Ratio Data Corresponding to Two Methods of Loss Determination for Turbine Build Number 1

Percent Cycle Time	Chosen Operating Conditions				Predicted Values of Efficiency and Corresponding Velocity Ratios							
					Turbine Loss Characteristics Determined by Revised Ainley Correlation				Turbine Loss Characteristics Determined by Modified Correlation			
	T_1 K	P_1 kPa	p_{13} kPa	U m/s	ν_{T1T13}	η_{T1T13} %	ν_{T1S13}	η_{T1S13} %	ν_{T1T13}	η_{T1T13} %	ν_{T1S13}	η_{T1S13} %
0·0	1069·1	405·6	101·4	246·5	0·450	81·34	0·416	69·43	0·450	81·68	0·416	69·71
4·9	1034·3	355·0	101·4	246·5	0·469	81·87	0·441	72·36	0·469	82·32	0·441	72·68
9·9	1001·2	311·3	101·4	246·5	0·493	82·55	0·469	74·94	0·493	83·13	0·469	75·39
14·8	969·7	273·7	101·4	246·5	0·522	83·31	0·502	77·18	0·522	84·01	0·502	77·78
19·7	939·6	241·0	101·4	246·5	0·559	84·11	0·542	79·00	0·559	84·90	0·542	79·65
24·6	910·9	212·7	101·4	246·5	0·606	84·87	0·590	80·30	0·607	85·55	0·590	80·89
29·6	883·5	188·1	101·4	246·5	0·669	85·51	0·650	80·86	0·669	85·63	0·650	80·96
33·0	865·1	173·3	101·4	246·5	0·724	85·79	0·701	80·62	0·724	84·99	0·701	79·87
34·5	833·8	173·3	101·4	246·5	0·738	85·92	0·714	80·56	0·738	84·80	0·714	79·51
39·4	751·2	173·3	101·4	246·5	0·780	86·21	0·753	80·21	0·780	83·94	0·753	78·11
44·3	691·2	173·3	101·4	246·5	0·817	86·37	0·785	79·75	0·817	82·88	0·785	76·55
49·3	645·4	173·3	101·4	246·5	0·848	86·45	0·812	79·25	0·848	81·72	0·812	74·93
54·2	609·3	173·3	101·4	246·5	0·876	86·48	0·836	78·74	0·876	80·51	0·836	73·32
59·1	580·1	173·3	101·4	246·5	0·901	86·48	0·857	78·24	0·900	79·30	0·857	71·75
64·0	555·8	173·3	101·4	246·5	0·923	86·47	0·875	77·74	0·922	77·88	0·875	70·09
69·0	535·4	173·3	101·4	246·5	0·943	86·43	0·892	77·26	0·943	76·88	0·892	68·74
73·9	518·1	173·3	101·4	246·5	0·961	86·39	0·906	76·83	0·961	75·74	0·906	67·36
78·8	503·1	173·3	101·4	246·5	0·978	86·35	0·920	76·42	0·978	74·65	0·920	66·06
83·7	490·1	173·3	101·4	246·5	0·993	86·30	0·932	76·02	0·993	73·60	0·932	64·82
88·7	478·6	173·3	101·4	246·5	1·007	86·25	0·943	75·64	1·007	72·59	0·943	63·65
93·6	468·5	173·3	101·4	246·5	1·020	86·20	0·953	75·28	1·020	71·63	0·953	62·55
98·5	459·5	173·3	101·4	246·5	1·032	86·14	0·962	74·94	1·032	70·71	0·962	61·51
100·0	457·0	173·3	101·4	246·5	1·035	86·12	0·965	74·82	1·035	70·44	0·965	61·21

TABLE VII

Variation of Flow Characteristics Throughout Pulsating-Flow Cycle–Build 1; Design Speed; Loss Characteristics Determined by Modified Correlation

Percent Cycle Time	T_1 K	P_1 kPa	m_0 g	$\Sigma\triangle m_{IN}$ g	$\Sigma\triangle m_{OUT}$ g	$\Sigma\triangle W_{IS}$ kJ	$\Sigma\triangle W_{ACT}$ kJ	ν_{T1S13}	η_{T1S13} %
0·0	1069·1	405·6	74·9	0·0	0·8	0·3	0·2	0·411	69·59
4·9	1034·3	355·0	67·8	0·0	7·8	2·7	1·9	0·436	72·21
9·9	1001·2	311·3	61·4	0·0	14·1	4·5	3·3	0·465	74·77
14·8	969·7	273·7	55·7	0·0	19·7	6·0	4·4	0·498	77·19
19·7	939·6	241·0	50·7	0·0	24·8	7·1	5·3	0·538	79·29
24·6	910·9	212·7	46·1	0·0	29·3	8·0	6·0	0·586	80·81
29·6	883·5	188·1	42·0	0·0	33·3	8·6	6·5	0·647	81·19
				End of Blowdown					
33·0	865·1	173·3	39·5	0·9	35·8	9·0	6·8	0·699	80·30
34·5	833·8	173·3	40·9	3·4	36·9	9·1	6·9	0·712	79·91
39·4	751·2	173·3	45·5	11·6	40·7	9·5	7·2	0·750	78·40
44·3	691·2	173·3	49·4	19·4	44·6	9·9	7·5	0·781	76·74
49·3	645·4	173·3	52·9	26·9	48·6	10·3	7·8	0·809	75·06
54·2	609·3	173·3	56·0	34·2	52·8	10·7	8·1	0·832	73·42
59·1	580·1	173·3	58·8	41·3	57·2	11·1	8·4	0·853	71·84
64·0	555·8	173·3	61·4	48·3	61·6	11·4	8·6	0·871	70·34
69·0	535·4	173·3	63·7	55·1	66·0	11·8	8·9	0·888	68·92
73·9	518·1	173·3	65·9	61·7	70·6	12·1	9·1	0·903	67·59
78·8	503·1	173·3	67·9	68·3	75·3	12·5	9·3	0·916	66·33
83·7	490·1	173·3	69·6	74·8	79·9	12·8	9·5	0·928	65·16
88·7	478·6	173·3	71·3	81·2	84·7	13·1	9·7	0·939	64·07
93·6	468·5	173·3	72·8	87·6	89·5	13·5	10·0	0·949	63·04
98·5	459·5	173·3	74·3	93·8	94·4	13·8	10·2	0·958	62·08
100·0	457·0	173·3	74·7	95·7	95·8	13·9	10·2	0·961	61·81

$U = 246{\cdot}5$ m/s. $p_{13} = 101{\cdot}4$ kPa. Mean Turbine Efficiency: $\bar{\eta}_{T1S13} = 73{\cdot}59\%$. Mean Turbine Inlet Temperature: $\bar{T}_{1(MASS)} = 720{\cdot}0$ K. $\bar{T}_{1(TIME)} = 705{\cdot}0$ K.

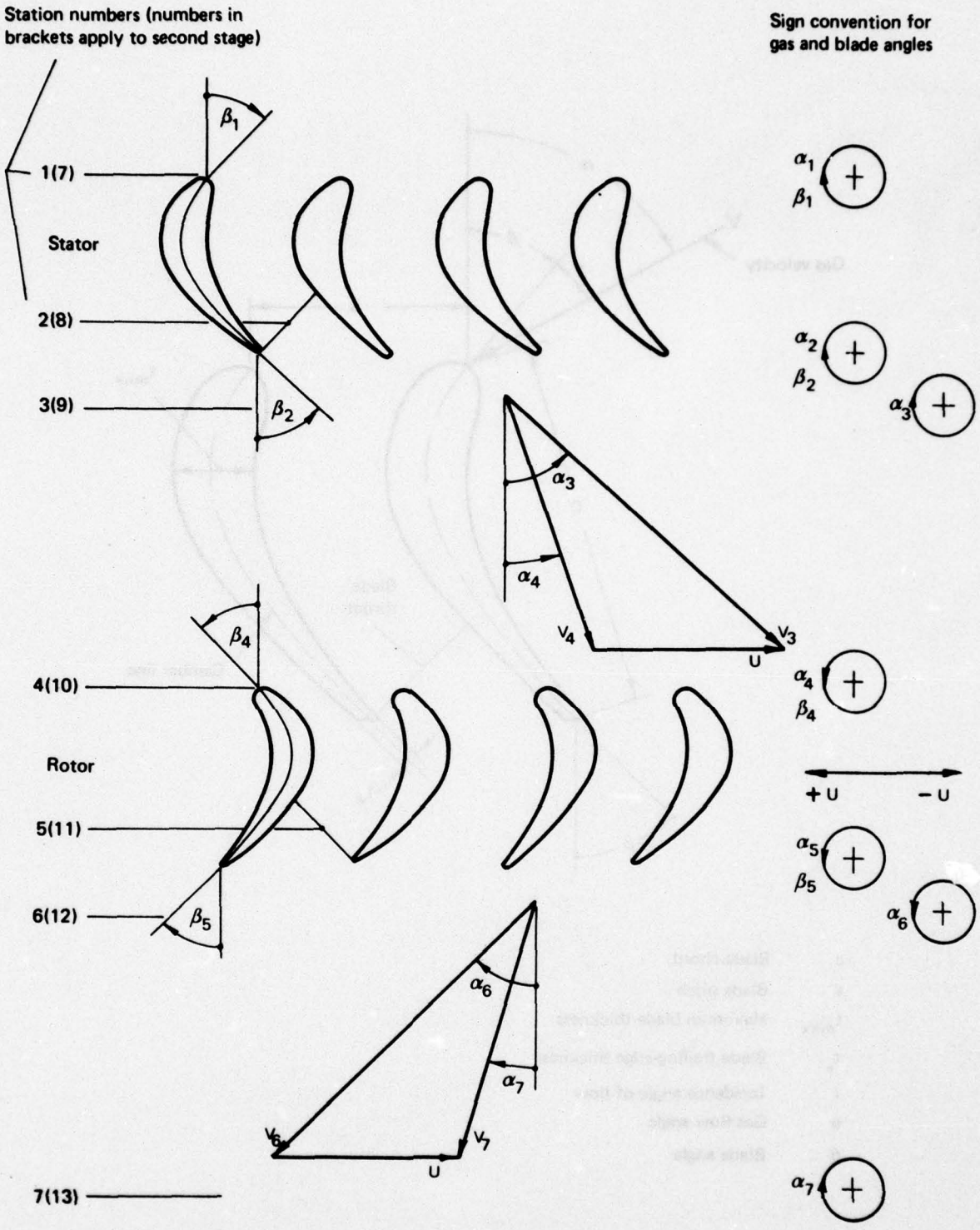

FIG. 1 DIAGRAMMATIC REPRESENTATION OF TURBINE STATOR AND ROTOR TOGETHER WITH VELOCITY DIAGRAMS

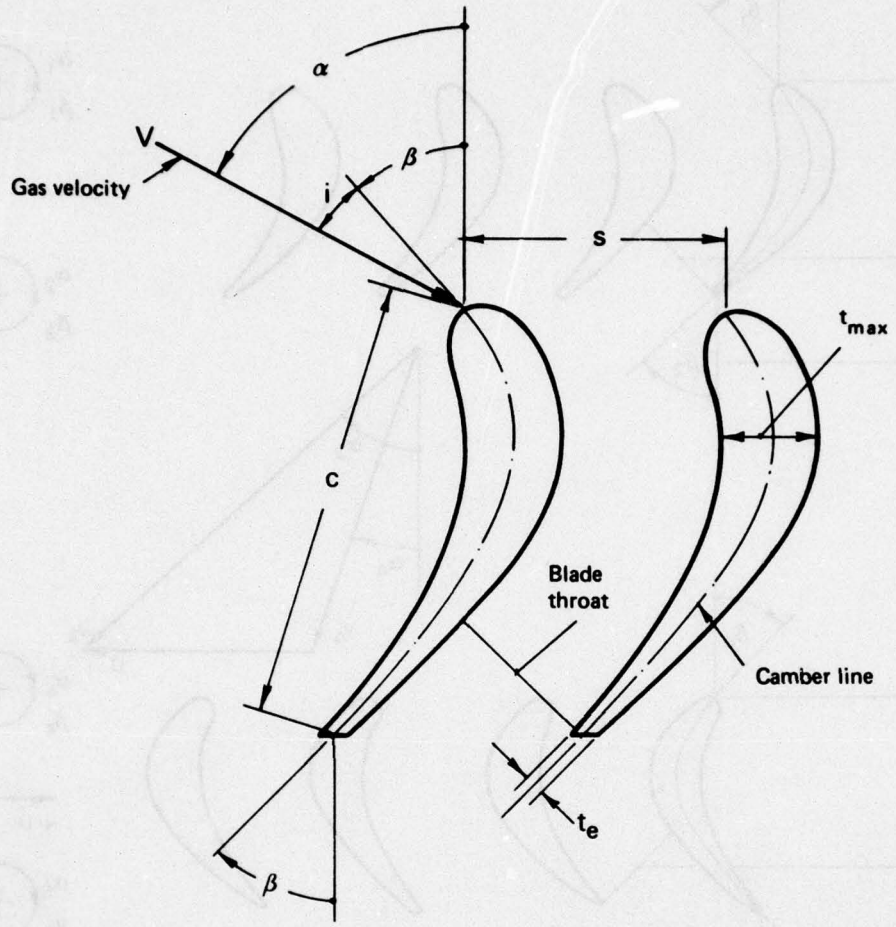

c	Blade chord
s	Blade pitch
t_{max}	Maximum blade thickness
t_e	Blade trailing-edge thickness
i	Incidence angle of flow
α	Gas flow angle
β	Blade angle

FIG. 2 TURBINE BLADE NOMENCLATURE

T6 profile on parabolic camber line – $t_{max}/c = 0.200$

Selected blade shape

Design-point velocity diagrams as selected in Section 2.1.1 together with design-point velocities as determined in Section 2.1.3

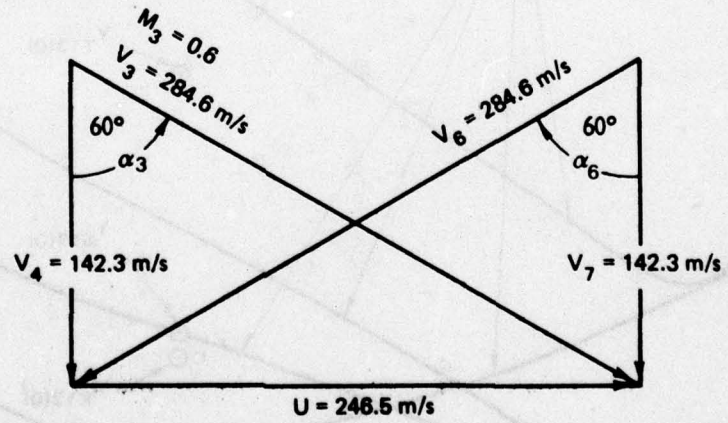

Design-point velocity diagrams

FIG. 3 SELECTED BLADE SHAPE AND DESIGN-POINT VELOCITY DIAGRAMS FOR THE SINGLE-STAGE TURBINE

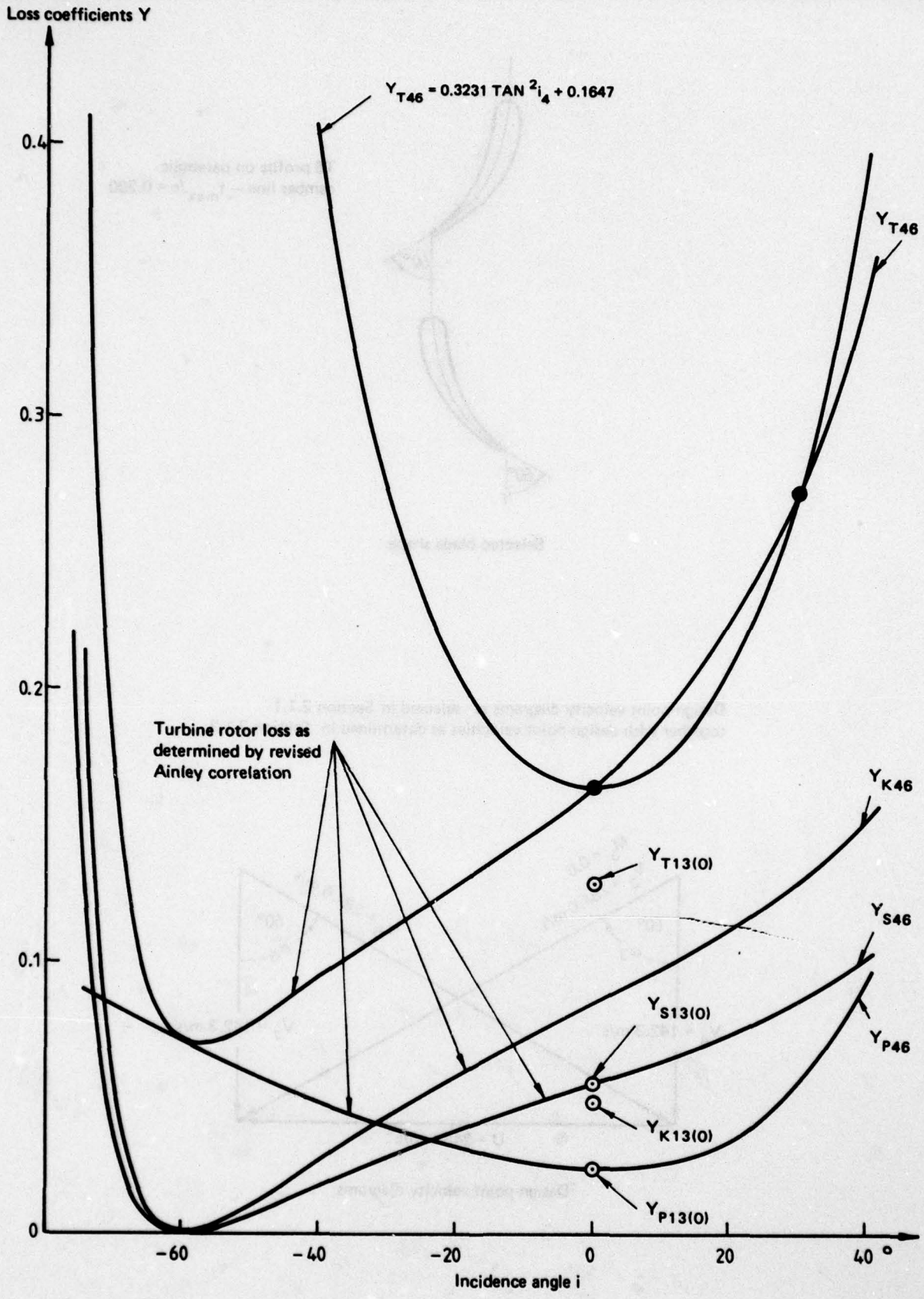

FIG. 4 VARIATION OF LOSS COEFFICIENTS WITH INCIDENCE ANGLE

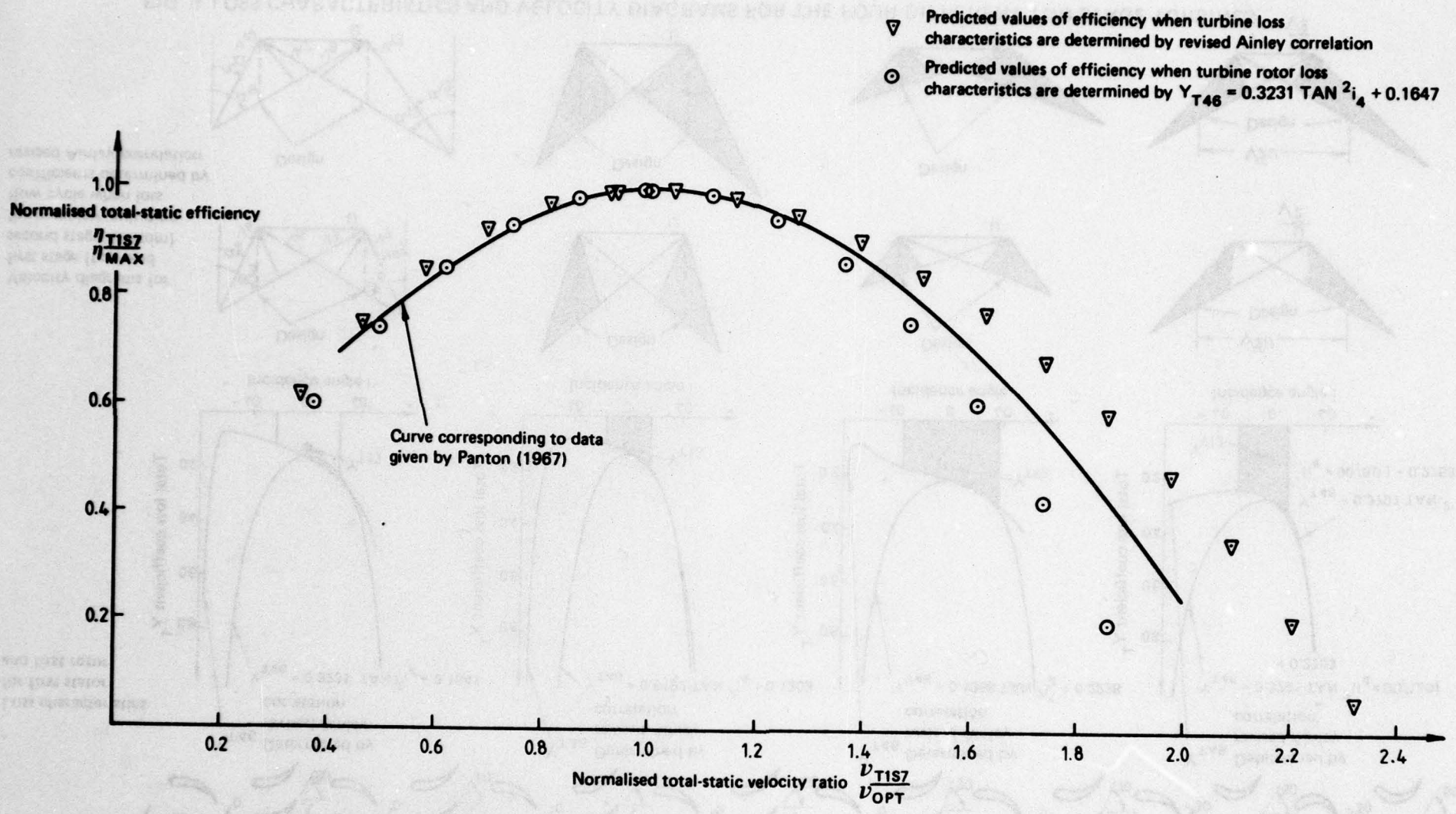

FIG. 5 PREDICTED VALUES OF EFFICIENCY COMPARED WITH EXPERIMENTAL DATA

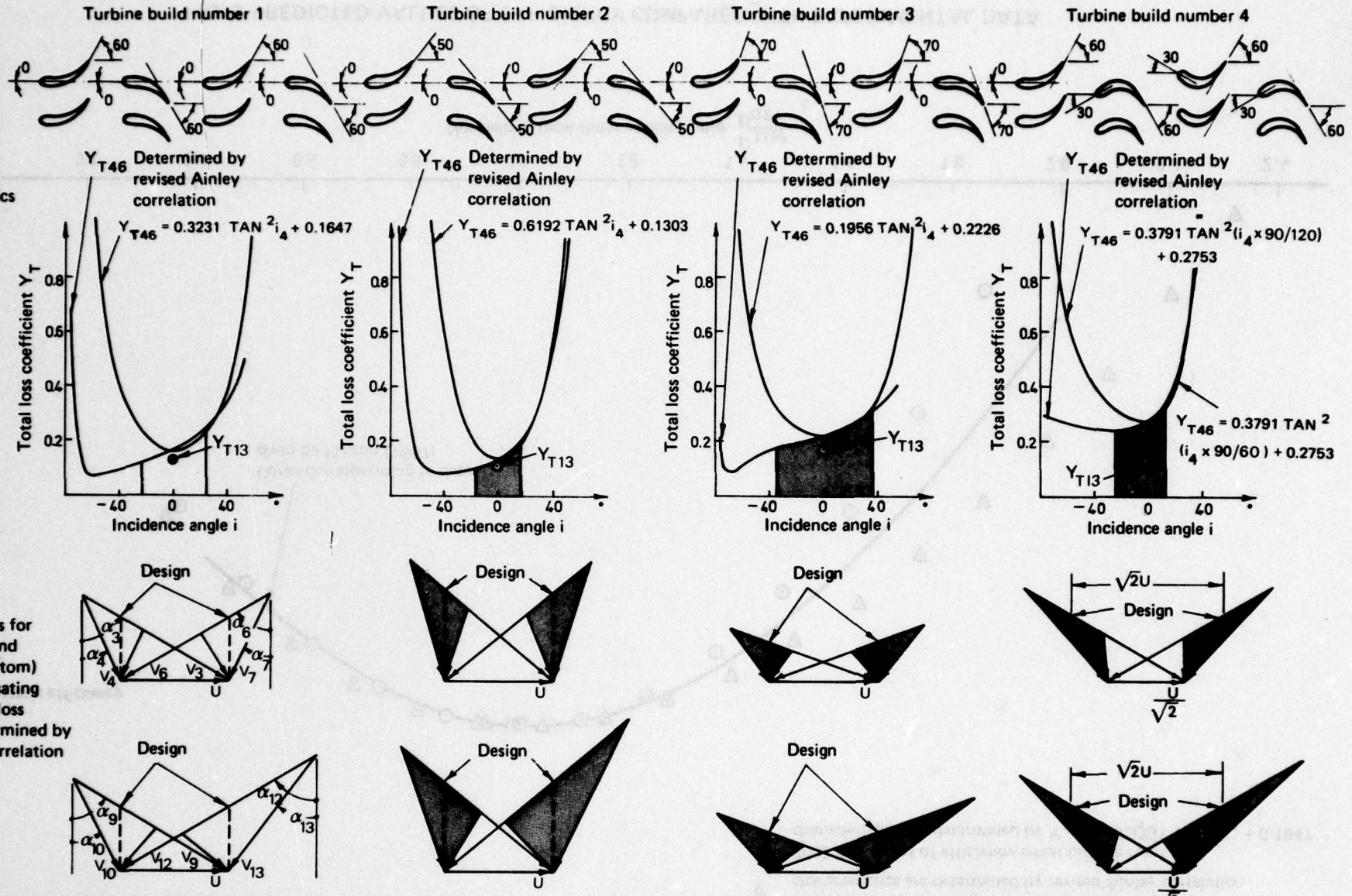

FIG. 6 LOSS CHARACTERISTICS AND VELOCITY DIAGRAMS FOR THE FOUR DIFFERENT TWO-STAGE TURBINES

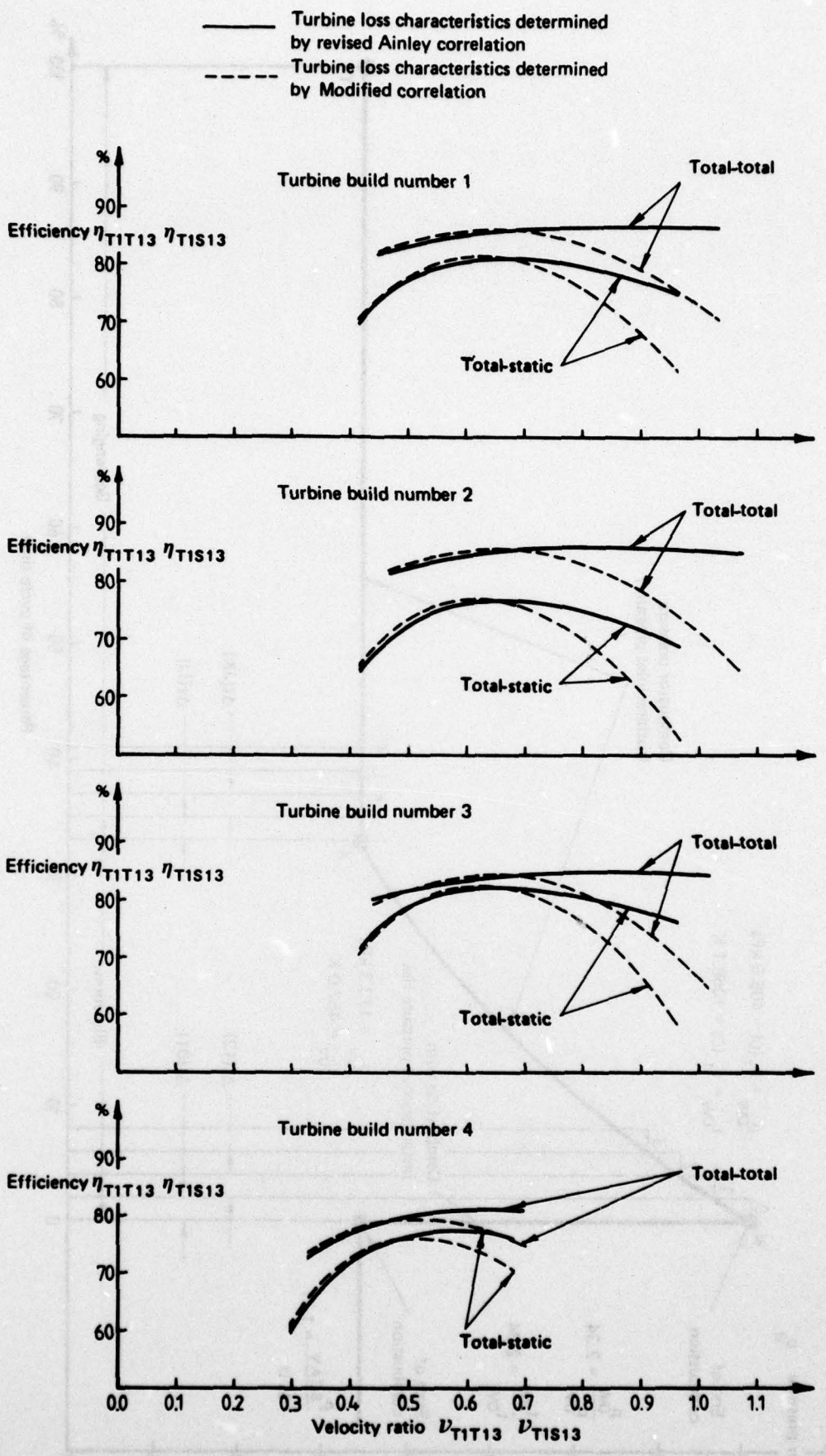

FIG. 7 EFFICIENCY-VELOCITY RATIO RELATIONSHIPS – BUILDS 1 TO 4; DESIGN SPEED; LOSSES DETERMINED BY BOTH REVISED AINLEY AND MODIFIED CORRELATIONS

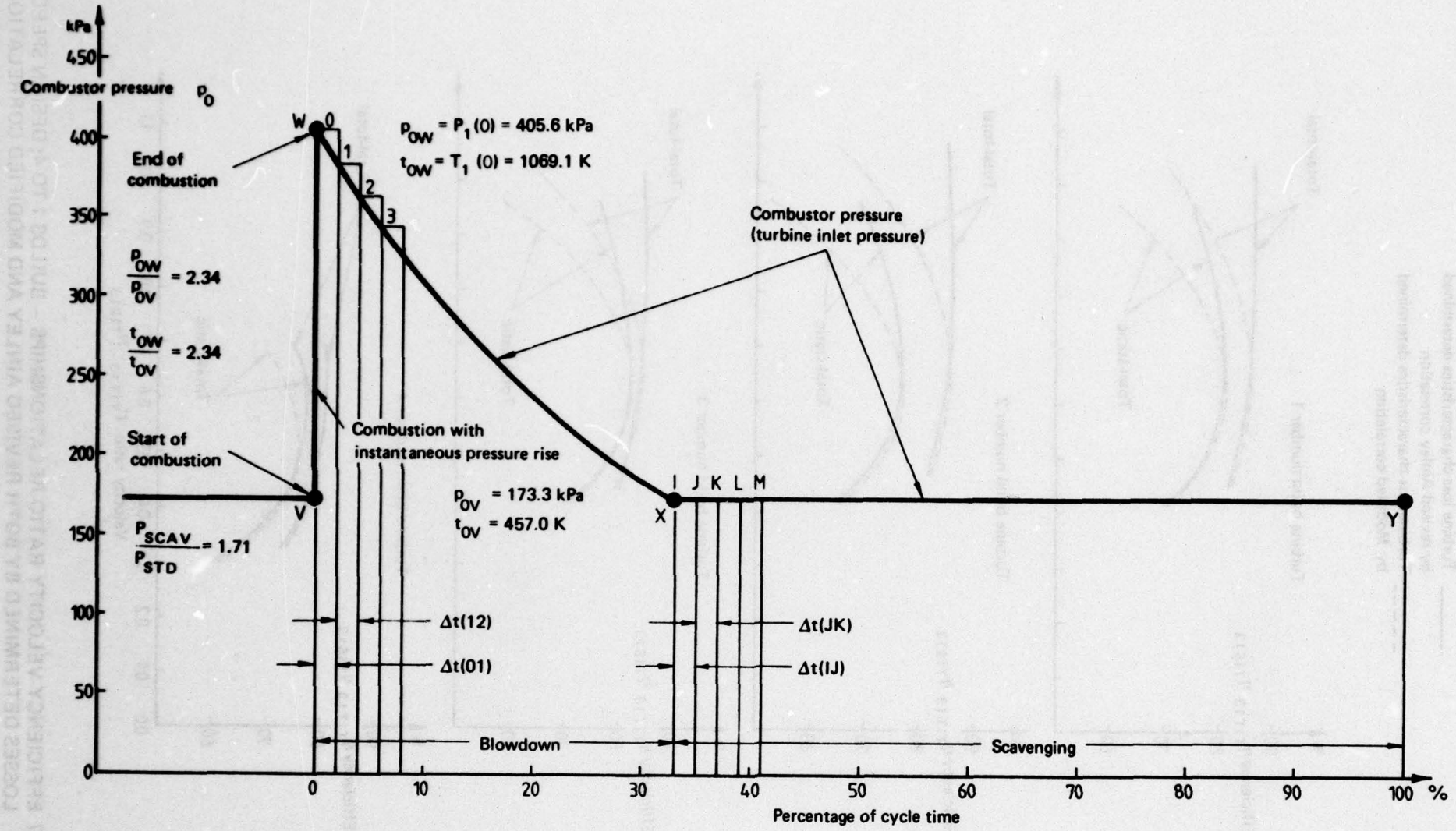

FIG. 8 IDEALISED PRESSURE PULSE USED IN PULSATING-FLOW ANALYSIS

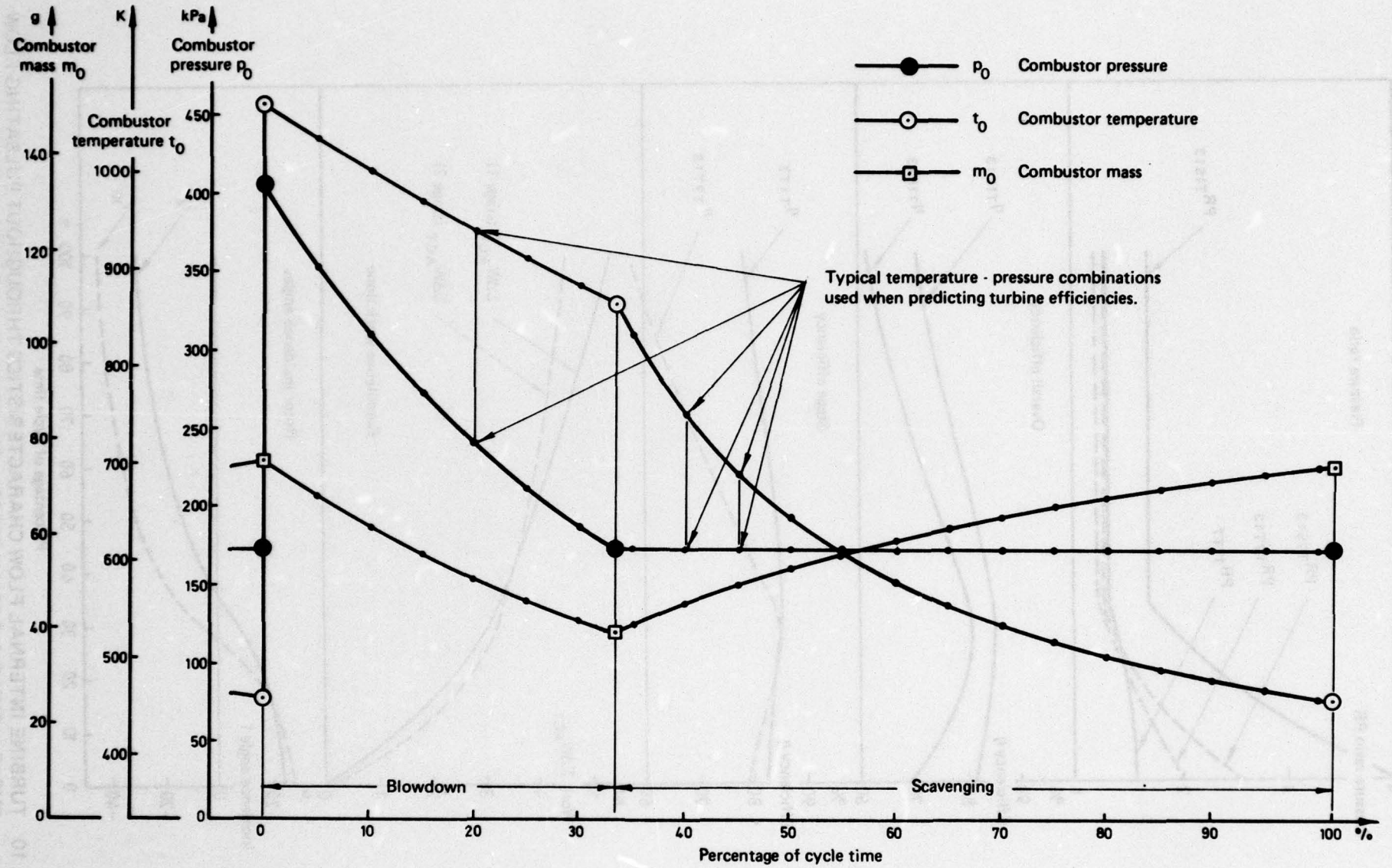

FIG. 9 COMBUSTOR PRESSURE, TEMPERATURE AND MASS THROUGHOUT PULSATING-FLOW CYCLE

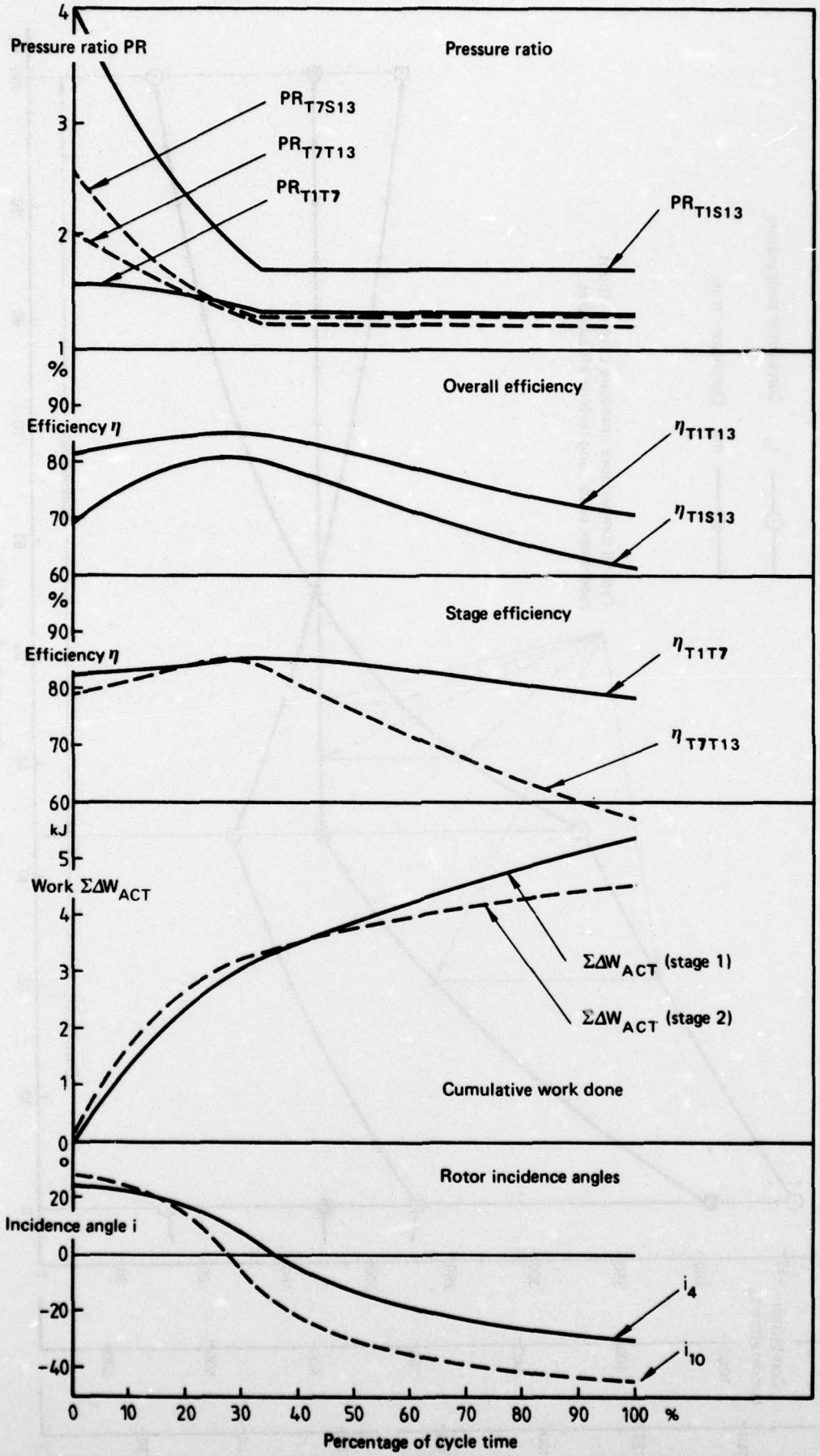

FIG. 10 TURBINE INTERNAL FLOW CHARACTERISTICS THROUGHOUT PULSATING-FLOW CYCLE – BUILD 1; DESIGN SPEED; LOSS CHARACTERISTICS DETERMINED BY MODIFIED CORRELATION

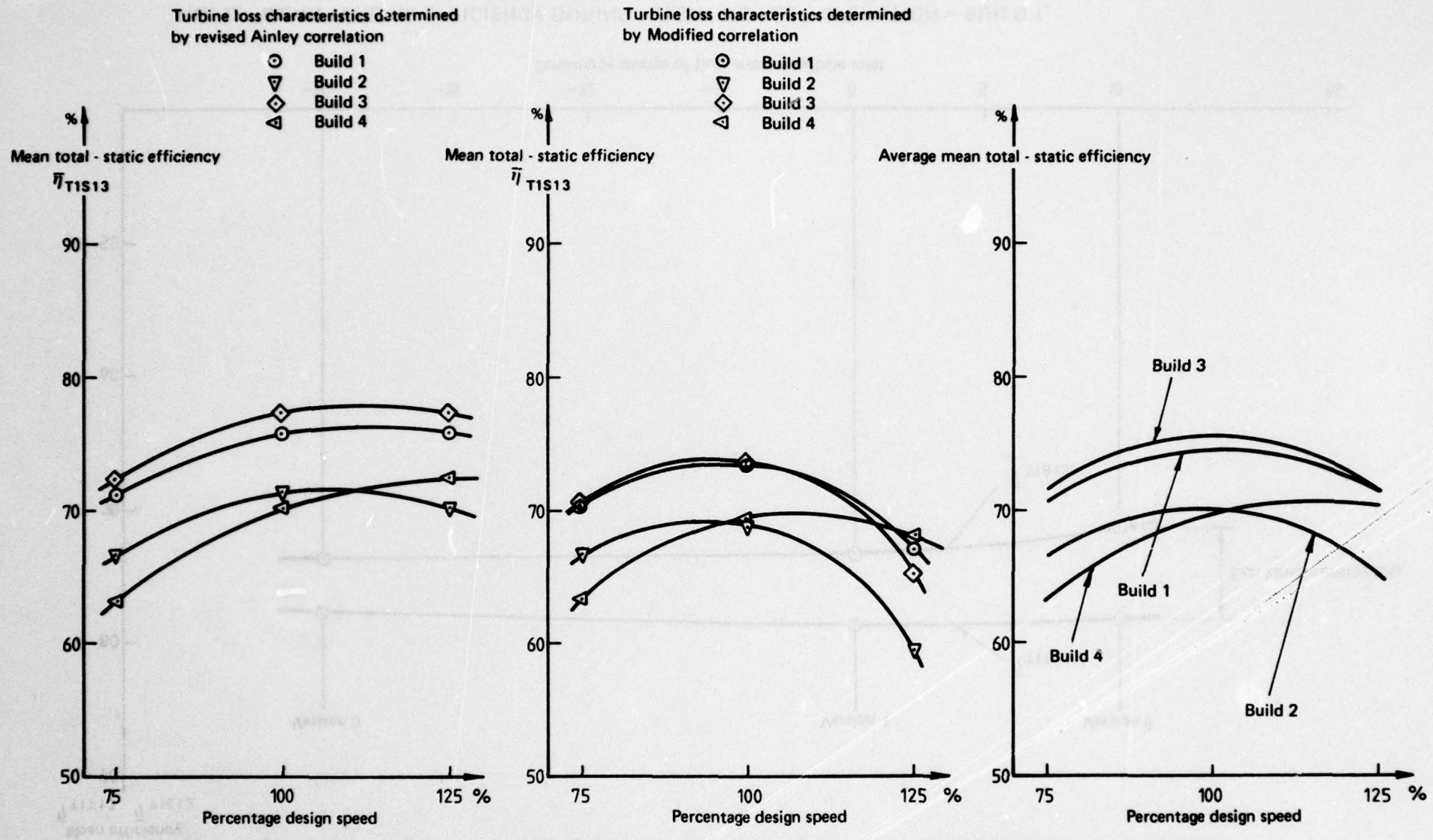

FIG. 11 MEAN TURBINE EFFICIENCY DURING PULSATING-FLOW OPERATION Vs SPEED FOR LOSSES DETERMINED BY BOTH REVISED AINLEY AND MODIFIED CORRELATIONS

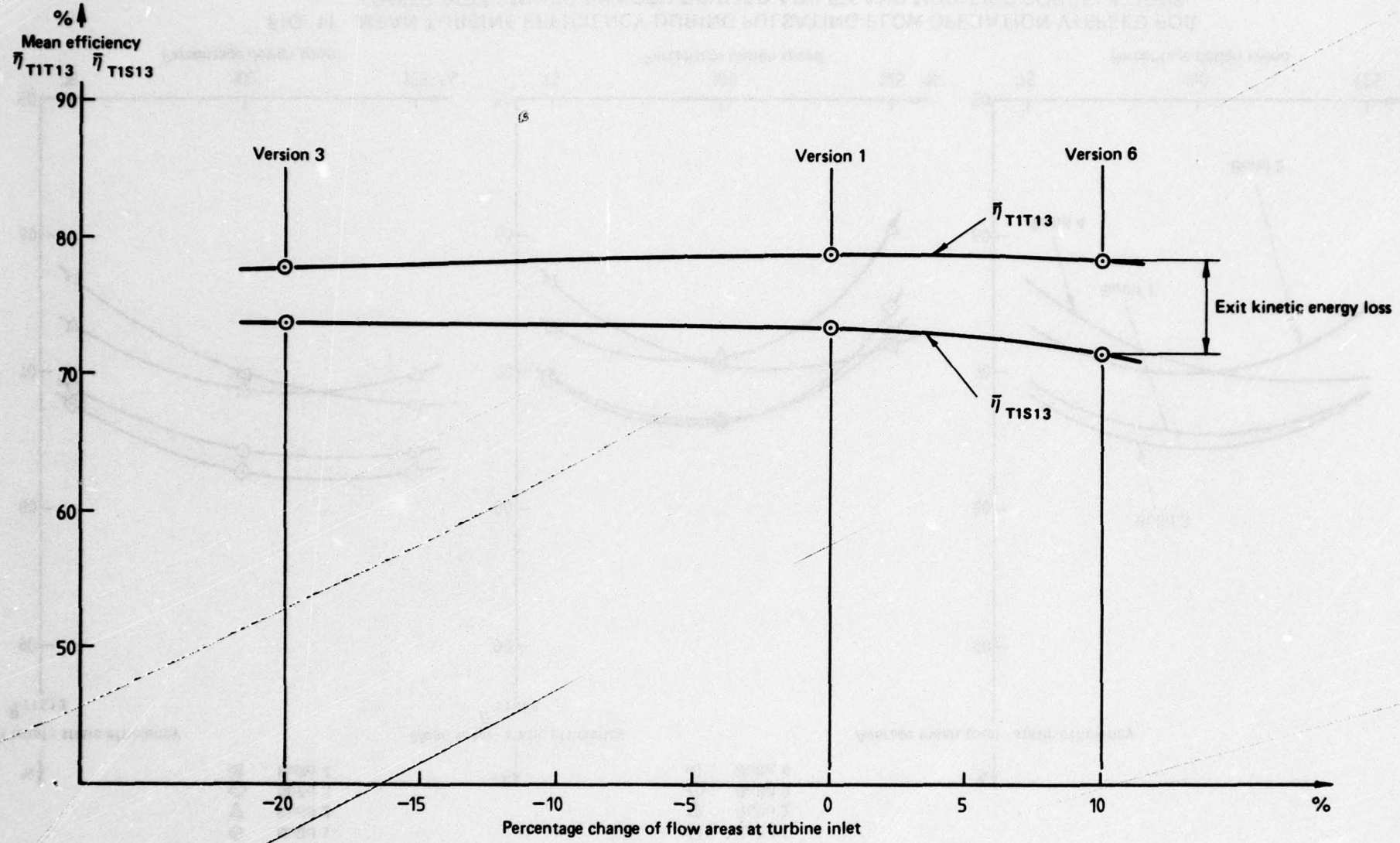

FIG. 12 MEAN TURBINE EFFICIENCY DURING PULSATING-FLOW OPERATION – BUILD 1, VERSIONS 1, 3 AND 6; BUILD 1 DESIGN SPEED; LOSSES DETERMINED BY MODIFIED CORRELATION

DISTRIBUTION

AUSTRALIA

	Copy No.
DEPARTMENT OF DEFENCE	
Central Office	
Chief Defence Scientist	1
Executive Controller, ADSS	2
Superintendent, Defence Science Administration	3
Defence Library	4
J.I.O.	5
Assistant Secretary, DISB	6–23
Aeronautical Research Laboratories	
Chief Superintendent	24
Superintendent — Mechanical Engineering	25
Divisional File — Mechanical Engineering	26
Author — Lincoln Erm	27
J. E. Williams	28
D. A. Frith	29
Library	30
Materials Research Laboratories	
Library	31
Weapons Research Laboratories	
Library	32
Air Office	
Air Force Scientific Adviser	33
Library, Engineering, CAFTS Branch	34
SENGSO, Support Command, H.Q.	35
Library, A.R.D.U. Edinburgh, Sth. Aust.	36
Army Office	
Army Scientific Adviser	37
Royal Military College	38
US Army Standardisation Group	39
Navy Office	
Naval Scientific Adviser	40
Central Studies Establishment	
Library	41

AUSTRALIA (cont.)

Engineering Development Establishment

Library 42

RAN Research Laboratory

Library 43

DEPARTMENT OF PRODUCTIVITY

Australian Government Engine Works
Mr. J. L. Kerin 44
Government Aircraft Factories
Library 45

DEPARTMENT OF NATIONAL RESOURCES

Secretary, Canberra 46

DEPARTMENT OF TRANSPORT

Director General/Library 47
Airworthiness Group (Mr. R. Ferrari) 48

STATUTORY, STATE AUTHORITIES AND INDUSTRY

Australian Atomic Energy Commission (Director) NSW 49
C.S.I.R.O. Central Library 50
C.S.I.R.O. Mechanical Engineering Division (Chief) 51
Gas & Fuel Corporation of Victoria (Research Director) 52
Ministry of Fuel and Power (Secretary) Victoria 53
S.E.C. Herman Research Laboratory (Librarian) Victoria 54
S.E.C. of Queensland, Library 55
Australian Coal Industry Research Labs Ltd, (Director) 56
BHP Central Research Laboratories, NSW 57
BHP Melbourne Research Laboratories 58
Commonwealth Aircraft Corporation (Manager) 59
Commonwealth Aircraft Corporation (Manager of Engineering) 60
Hawker de Havilland Pty Ltd (Librarian) Bankstown 61
Hawker de Havilland Pty Ltd (Manager) Lidcombe 62
Rolls Royce of Australia Pty Ltd (Mr. Mosley) 63

UNIVERSITIES AND COLLEGES

Adelaide	Barr Smith Library	64
	Professor of Mechanical Engineering	65
Australian National	Library	66
Flinders	Library	67
James Cook	Library	68
La Trobe	Library	69
Melbourne	Engineering Library	70
	Professor P. N. Joubert, Mechanical Engineering	71
	Mr. W. W. S. Charters	72
Monash	Library	73
	Professor I. J. Polmear, Materials Engineering	74
	Professor W. Melbourne	75
Newcastle	Library	76
	Professor I. Stewart, Chemical Engineering	77

AUSTRALIA (cont.)

		Copy No.
New England	Library	78
New South Wales	Physical Sciences Library	79
	Professor R. A. A. Bryant, Mechanical and Industrial Engineering	80
	Professor P. T. Fink, Mechanical and Industrial Engineering	81
	Assoc. Professor N. Y. Kirov, Fuel Technology	82
	Assoc. Professor R. W. Traill-Nash, Structural Engineering	83
	Professor A. H. Willis, Mechanical and Industrial Engineering	84
Queensland	Library	85
	Professor A. F. Pillow, Applied Mathematics	86
Sydney	Professor G. A. Bird, Aeronautical Engineering	87
	Professor J. W. Roderick, Mechanical Engineering	88
	Professor R. I. Tanner, Mechanical Engineering	89
	Professor R. Wilson, Applied Mathematics	90
Tasmania	Engineering Library	91
	Professor A. R. Oliver, Civil and Mechanical Engineering	92
	Dr. G. J. Walker, Civil and Mechanical Engineering	93
Western Australia	Library	94
	Professor Allen-Williams, Mechanical Engineering	95
	Dr. P. B. Chapman, Mathematics	96
RMIT	Library	97
	Mr. H. Millicer, Aeronautical Engineering	98
	Mr. Pugh, Mechanical Engineering	99
N.S.W. Institute of Technology	Professor J. P. Gostelow	100

CANADA

CAARC Co-ordinator Propulsion	101
Energy, Mines and Resources Department, Canadian Combustion Research Laboratories (Mr. B. Mitchell, Manager)	102
NRC, National Aeronautics Establishment, Library	103
NRC, Division of Mechanical Engineering (Dr. D. McPhail, Director)	104
NRC, Division of Mechanical Engineering, Gas Dynamics Laboratory (Mr A. Bachmeier)	105

UNIVERSITIES

McGill	Library	106
Toronto Institute of Aerophysics		107

FRANCE

AGARD, Library	108
Gaz de France, Library	109
Institute Francais de Petrole, Library	110
ONERA, Library	111
Service de Documentation, Technique de l'Aeronautique	112

GERMANY

ZLDI	113

INDIA

CAARC Co-ordinator Propulsion	114
Civil Aviation Department (Director)	115

		Copy No.
Defence Ministry, Aero Development Establishment, Library		116
Gas Turbine Research Establishment (Director)		117
Hindustan Aeronautics Ltd, Library		118
Indian Institute of Science, Library		119
Indian Institute of Technology, Library		120
National Aeronautical Laboratory (Director)		121
ISRAEL		
Technion—Israel Institute of Technology (Professor J. Singer)		122
ITALY		
Associazione Italiana di Aeronautica and Astronautica (Professor A. Evla)		123
JAPAN		
National Aerospace Laboratory, Library		124
UNIVERSITIES		
Tohuku (Sendai)	Library	125
Tokyo	Institute of Space and Aerospace	126
NETHERLANDS		
Central Organization for Applied Science Research in the Netherlands TNO, Library		127
National Aerospace Laboratory (NLR), Library		128
NEW ZEALAND		
Air Department, R.N.Z.A.F. Aero Documents Section		129
Transport Ministry, Civil Aviation Division, Library		130
UNIVERSITIES		
Canterbury	Library	131
	Professor D. Stevenson, Mechanical Engineering	132
	Mr. F. Fahy, Mechanical Engineering	133
	Mr. J. Stott, Chemical Engineering	134
Christchurch	Dr. D. Lindley, Mechanical Engineering	135
SWEDEN		
Aeronautical Research Institute		136
Chalmers Institute of Technology, Library		137
Kungl. Tekniska Hogscholens		138
SAAB, Library		139
Research Institute of the Swedish National Defence		140
SWITZERLAND		
Brown Boverie (Management Chairman)		141
Escher — Wyss Ltd (Manager)		142
Institute of Aerodynamics E.T.H.		143
Institute of Aerodynamics (Professor J. Ackeret)		144
Sulzer Bros. Ltd (General Manager)		145

Copy No.

UNITED KINGDOM

Australian Defence Science and Technical Representative	146
Mr A. R. G. Brown ADR/MAT (MEA)	147
Ministry of Power (Chief Scientist)	148
Aeronautical Research Council, N.P.L. (Secretary)	149
CAARC N.P.L. (Secretary)	150
Royal Aircraft Establishment Library, Farnborough	151
Royal Aircraft Establishment Library, Bedford	152
C.A.T.C. Secretariat	153
Military Vehicles Engineering and Experimental Establishment	154
National Engineering Laboratories (Superintendent)	155
National Gas Turbine Establishment (Director)	156
National Industrial Fuel Efficiency Services (Director)	157
British Library, Science Reference Library	158
British Library, Lending Division	159
CAARC Co-ordinator, Propulsion	160

INDUSTRY

Aircraft Research Association, Library	161
C. A. Parsons, Library	162
C. A. Parsons Gas Turbine Department Library	163
Central Electricity Generating Board	164
English Electric Co. Ltd. Gas Turbine Department (Dr. W. Rizk)	165
Energy Conversion Ltd (Research Director)	166
Fulmer Research Institute Ltd (Research Director)	167
Lucas Gas Turbine Equipment (Director)	168
Motor Industries Research Association (Director)	169
Ricardo H. Co. (Manager)	170
Rolls-Royce (1971) Ltd, Aeronautics Division (Chief Librarian)	171
Ruston & Hornsby, Turbine Division, (Mr. A. V. Jackman)	172
Science Museum Library	173

AIRCRAFT COMPANIES

Hawker Siddeley Aviation Ltd, Brough	174
Hawker Siddeley Aviation Ltd, Greengate	175
Hawker Siddeley Aviation Ltd, Kingston-upon-Thames	176
Hawker Siddeley Dynamics Ltd, Hatfield	177
British Aircraft Corporation (Holdings) Ltd, Commercial Aircraft Division	178
British Aircraft Corporation (Holdings) Ltd, Military Aircraft	179
British Aircraft Corporation (Holdings) Ltd, Commercial Aviation Division	180
British Hovercraft Corporation Ltd (E. Cowes)	181
Fairey Engineering Ltd, Hydraulic Division	182
Short Brothers & Harland	183
Westland Helicopters Ltd	184

UNIVERSITIES AND COLLEGES

Bristol	Library, Engineering Department	185
Cambridge	Library, Engineering Department	186
	Professor G. K. Batchelor	187
	Sir William Hawthorne	188
	Sir James Lighthill	189
Liverpool	Fluid Mechanics Department	190
London	Professor A. D. Young, Queen's College	191

Manchester	Professor N. Johannessen	192
Nottingham	Library	193
Salford	Dr. J. H. Horlock	194
Sheffield	Library Department of Fuel Technology	195
Southampton	Library	196
Strathclyde	Library	197
Cranfield Institute of Technology	Library	198
	Professor Lefebvre	199
Imperial College	The Head	200
	Professor of Mechanical Engineering	201
	Professor B. G. Neal	202

UNITED STATES OF AMERICA

Counsellor, Defence Science	203
N.A.S.A. Scientific and Technical Information Facility	204
Sandia Group (Research Organisation)	205
American Institute of Aeronautics and Astronautics	206
Applied Mechanics Reviews	207
The John Crerar Library	208
Allis Chalmers Inc., (Director)	209
Boeing Co. Head Office	210
Cessna Aircraft Co. (Mr. D. W. Mallonee, Executive Engineer) (Structures only)	211
Esso Research Laboratories (Director)	212
General Electric (Aircraft Engine Group)	213
Lockheed Aircraft Co. (Director)	214
Monsanto Co. (Director)	215
McDonnell Douglas Corporation (Director)	216
Westinghouse Laboratories (Director)	217
United Technologies Corporation, Fluid Dynamics Laboratories	218
United Technologies Corporation, Pratt and Whitney Aircraft Group Dr. A. A. Mikalajczak	219
Battelle Memorial Institute, Library	220

UNIVERSITIES AND COLLEGES

California	Department of Aerosciences	221
Cornell (New York)	Library, Aeronautical Laboratories	222
Florida	Department of Aeronautical Engineering	223
Harvard	Professor A. F. Carrier, Division of Engineering and Applied Mathematics	224
	Dr. S. Goldstein, Division of Engineering and Applied Physics	225
Johns Hopkins	Professor S. Corrsin, Department of Mechanical Engineering	226
Illinois	Talbot Laboratories	227
Princeton	Professor G. L. Mellor	228
Stanford	Library, Department of Aeronautics	229
George Washington	Professor Fruedenthal	230
Brooklyn	Library, Polytech Aeronautical Laboratories	231
California	Library, Guggenheim Aeronautical Laboratories	232
Iowa State University of Science and Technology	Professor G. K. Sekovy	233
Pennsylvania State	Professor B. Lakshminarayana	234
Texas A & M.	Dr. M. D. Boyce	235

Spares 236–255